TASK ALLOCATION FOR NETWORKED AUTONOMOUS UNDERWATER VEHICLES

BY INDRANEEL S. KULKARNI

A thesis submitted to the

Graduate School—New Brunswick

Rutgers, The State University of New Jersey

in partial fulfillment of the requirements

for the degree of

Master of Science

Graduate Program in Electrical and Computer Engineering

Written under the direction of

Prof. Dario Pompili

and approved by

____

____

____

New Brunswick, New Jersey

May, 2010

© 2010
Indraneel S. Kulkarni
ALL RIGHTS RESERVED

ABSTRACT OF THE THESIS

Task Allocation for Networked Autonomous Underwater Vehicles

by Indraneel S. Kulkarni

Thesis Director: Prof. Dario Pompili

Underwater Acoustic Sensor Networks (UW-ASNs) consist of stationary or mobile nodes such as Autonomous Underwater Vehicles (AUVs), which may be classified as propeller-driven vehicles and gliders, that are equipped with a variety of sensors for performing collaborative monitoring tasks. UW-ASNs are envisioned for missions like oceanographic data collection, ocean sampling, offshore exploration, disaster prevention, tsunami and seaquake warning, assisted navigation, distributed tactical surveillance, and mine reconnaissance. A task allocation and optimization framework for networked AUVs that participate as a team to accomplish such missions is developed in this work. These missions entrusted to the AUVs are sometimes critical to human life and property, are bound by severe time and energy constraints, and involve a high degree of inter-vehicular communication. The objective of the framework is to form the best possible team, which is a subset of all deployed AUVs that is best suited to accomplish the mission, while adhering to the constraints. Successful completion of the mission is dependent on effective communication between the networked AUVs and to achieve this a geocasting based networking framework is also proposed.

Research specific to this area has been limited. Hence, a framework based on energy minimization for the team of AUVs to complete the mission in given time bound is proposed. Further, the effect of size of geocast region, effect of underwater current on the choice of geocast region and on localized nature of the problem, and the performance of Propeller Driven Vehicles (PDVs) and gliders is compared.

Acknowledgements

It has been a long two and half year journey to my masters dissertation and I would like to acknowledge several people for their support. I am indebted to my mother and late father for their constant encouragement and unconditional support, without whom this journey would not be possible.

I would like to thank my thesis advisor Prof. Dario Pompili for the excellent guidance, motivation to do research and implement innovative ideas throughout the course of thesis. Because of his insight, constant support and guidance, I could publish two papers in WUWNet08 and IEEE JSAC's special issue on mission critical networking. His constructive criticism has helped me hone my technical writing skills and has imbibed in me the meticulousness required to accomplish quality work.

I am grateful to The Mathworks for providing me the opportunity to intern with them. I would like to thank my managers Mr. Rob Purser and Ms. Sherryl Radbil for the invaluable experience gained under their guidance. Thanks to Mr. Alan Weiss for guiding me in using the Optimization Toolbox to implement the task allocation algorithm in MATLAB. Also, thanks to Ankit Desai, Dilip Hari and Gautam Vallabha my coworkers for participating in useful brainstorming discussions and continuous guidance throughout.

I was lucky to have wonderful roommates in Siddharth, Jay and Prashant and very helpful labmates in John Paul, Eun Kyung and Hari. I would also like to thank my friends back home for constant encouragement through out the course of my M.S. Also, thanks to Ms. Meher Sidhwa for helping in proof reading and refining the WUWNet08 paper.

Thanks to Dr. Zoran Gajic and Prof. Manish Parashar for accepting to be on my defense committee.

I would like to thank my mentors Mr. Prashant Chitnis and Ms. Varsha Pradhan. Special thanks to Mr. Purshottam Gupte, Ms. Rohini Gupte, Ms. Kusum Chitnis, Mr. Arvind Karnik, Mr. Mandar Kulkarni and Ms. Swapna Kulkarni for their kind support.

I thank all the faculty and staff of ECE department at Rutgers for their help and support.

Dedication

To my mother ***Mrs. Prabha S. Kulkarni*** *and*
late father ***Mr. Surendra W. Kulkarni****.*

Table of Contents

List of Figures

Chapter 1
Introduction

Underwater sensor networks have enabled us to explore the ocean extensively, and enhanced our ability to observe and predict its behavior. The advent of underwater sensor networks has empowered us to monitor the ocean over longer duration and with higher resolution. The underwater sensor networks that use acoustic waves to communicate are known as Underwater Acoustic Sensor Networks (UW-ASNs) [7]. For efficient operation of UW-ASNs it is necessary to have an optimal task allocation mechanism for the sensor nodes. In this work we envision the use of Autonomous Underwater Vehicles (AUVs) as mobile sensor nodes in an UW-ASN, which have underwater acoustic communication capability.

This chapter is organized as follows; in Sect. 1.1 we describe the UW-ASNs and their applications in detail, in Sect. 1.2 we present an overview of various types of AUVs that can be used to form an UW-ASN, in Sect. 1.3 we highlight the importance and need for networking between the AUVs and the geocast protocol proposed, and in Sect. 1.4 we present an overview of the entire thesis.

1.1 Underwater Acoustic Sensor Networks (UW-ASNs) and their Applications

Underwater Acoustic Sensor Networks consist of stationary or mobile nodes such as Autonomous Underwater Vehicles, which comprise of Propeller Driven Vehicles (PDVs) and gliders, that are equipped with a variety of sensors for performing collaborative monitoring tasks as shown in Fig. 1.1 [36]. UW-ASNs are envisioned for applications like oceanographic data collection, ocean sampling, offshore exploration, distributed tactical surveillance, mine reconnaissance, tsunami and seaquake warning, surveillance of leakage in underwater oil and gas pipelines, data cables and submarine rescue. Failure of some of these missions would pose a threat to human life and property [41]. For example, the loss of human life

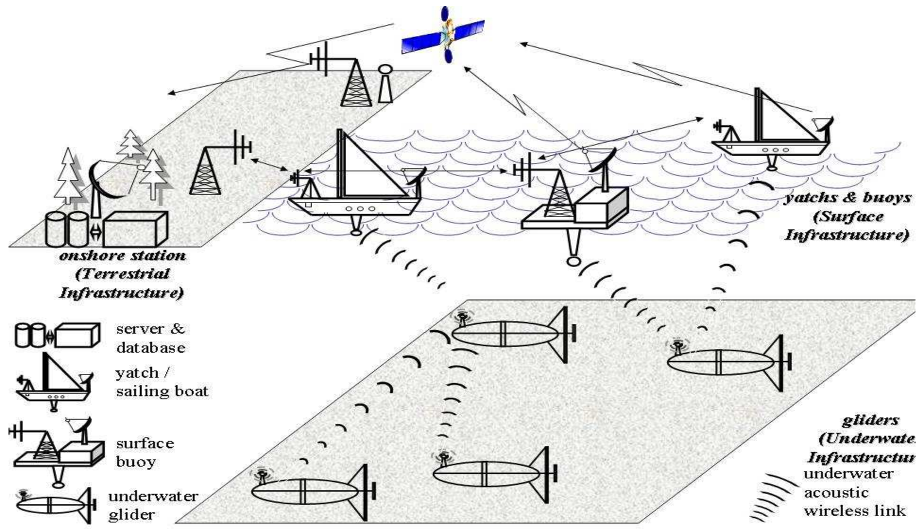

Figure 1.1: Underwater Acoustic Sensor Networks (UW-ASN) with Autonomous Underwater Vehicles (AUVs) as mobile nodes.

and property due to tsunami, blowing up of underwater oil pipeline or drowning of a nuclear powered submarine and its crew, is colossal. Missions, which involve safeguarding of life and property are essential for the safety, security, and economic vitality in a complex world characterized by uncertainty. Success of these missions is based on reliable and timely response by the rescue team to an untoward situation. The rescue team for such a timely response envisaged in this work is formed by networked AUVs.

1.2 Autonomous Underwater Vehicles (AUVs)

There are two categories of vehicles that can operate as AUVs, Propeller Driven Vehicles (PDVs) and gliders. PDVs are propeller driven, battery operated vehicles with high maneuverability and variable speed. There are two classes of PDVs, autonomously operated as shown in Figs. 1.2 and 1.3 [2] and Remotely Operated Vehicles (ROVs) as shown in Fig. 1.4 [5, 4]. ROVs are highly maneuverable underwater robots connected to surface vessel by umbilical cable and operated by a person aboard it. *The length of the cable confines the scope of operation of ROVs and human limitations of the operator, limit the mission length.* PDVs are autonomous vehicles that can operate without any external control once assigned a task.

The second category is underwater gliders, which are buoyancy-driven vehicles that alternately reduce and expand displaced volume to dive and climb through the ocean [39, 17]

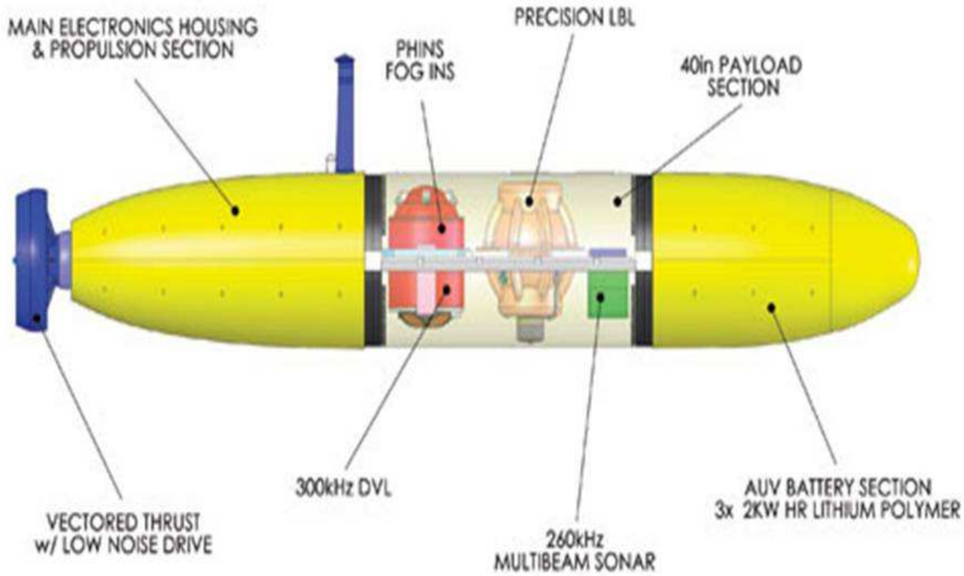

Figure 1.2: Construction of autonomous Propeller Driven Vehicle (PDV).

as shown if Figs. 1.5 and 1.6 [9, 3, 24, 1]. These vehicles are designed to glide from the ocean surface to its bottom and back while taking different measurements along a sawtooth trajectory through water [21]. Underwater gliders offer a solution for exploring the ocean with much higher resolution in space and time than is possible with techniques reliant on ships and moorings. Gliders cannot vary their speed substantially and are less maneuverable as compared to PDVs. However, although PDVs are time efficient means of ocean exploration due to their variable speed, they have a mission length limited to a few days due to high energy consumption. Gliders are in general slower than PDVs but they offer an energy-efficient solution for exploring the ocean in prolonged-time monitoring missions. There are two distinct advantages of speed and energy efficiency offered by PDVs and gliders respectively. In critical missions, in fact, PDVs may act as *primary responders*, whereas gliders may act as *sentinels*. As a team, the AUVs need to perform various tasks and measure different quantities for which they are fitted with a variety of sensors. Space, weight,

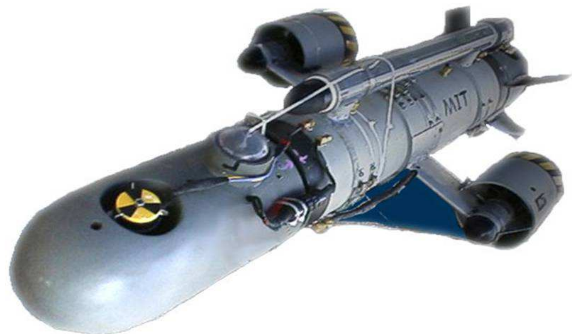

Figure 1.3: Autonomous PDVs.

Figure 1.4: Remotely Operated Vehicles (ROVs).

energy consumption, and other design constraints of AUVs limit the number of sensors a single AUV can carry. Due to this each AUV is fitted with a different set of sensors for gathering a variety of data. Hence, in order to take full advantage of the different design characteristics of PDVs and gliders, fitted with a variety of sensors, we envisage the use of a heterogenous team involving both types of vehicles.

1.3 Time Critical Networking

Missions involving multiple AUVs become feasible only if the vehicles communicate with each other effectively, as it is not possible for a team to collaborate otherwise [33, 31]. Communication is considered to be the critical link on which the success or failure of the mission depends. The task allocation and team formation process involves sharing of information

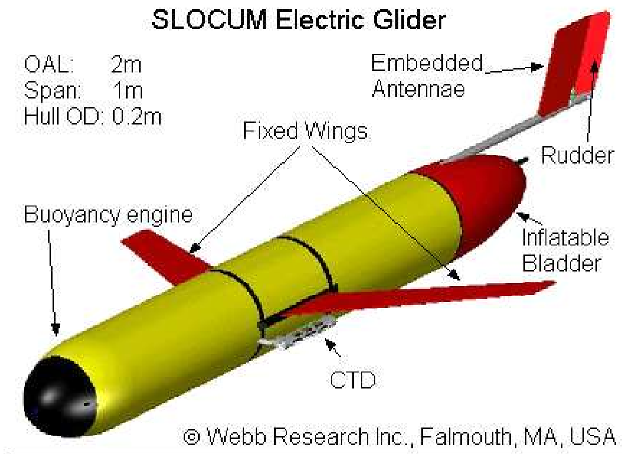

Figure 1.5: Underwater glider

about the positions of AUVs, ocean currents, available energy, sensors available onboard and the type of vehicle, i.e., PDV or glider. For energy efficient inter AUV communication we propose the use of geocasting protocol [8]. Geocasting in wireless sensor networks and adhoc networks is the delivery of a message from a source to all the nodes in a chosen geographical region [25, 26]. The shape of the geocast region is of vital importance for the efficient implementation of the protocol. The query packets transmitted, contain information about the shape of the geocast region, its center and its dimensions. The nodes receiving these query packets, knowing their own geographical location and information in the query packet can determine if they lie in the geocast region and if they should be responding to the query packet. All the nodes that lie inside the geocast region, when they receive the query packet, follow the geocasting protocol for query dissemination inside the region; as described in Sect. 3.2. If nodes lying outside the region receive the query packet, they discard it. The dissemination of query packet helps determine the number of nodes present inside the geocast region. Our work leverages this information while performing task allocation, as the geocasting protocol provides the superset of deployed AUVs for the optimization problem. This critical information exchange based on the geocasting protocol, mandatory to form the team, is shared using acoustic communication. From the task allocation and team formation process we infer that it is communication intensive and involves substantial amount of data exchange; hence, the idea of inter AUV networking is backbone of this work.

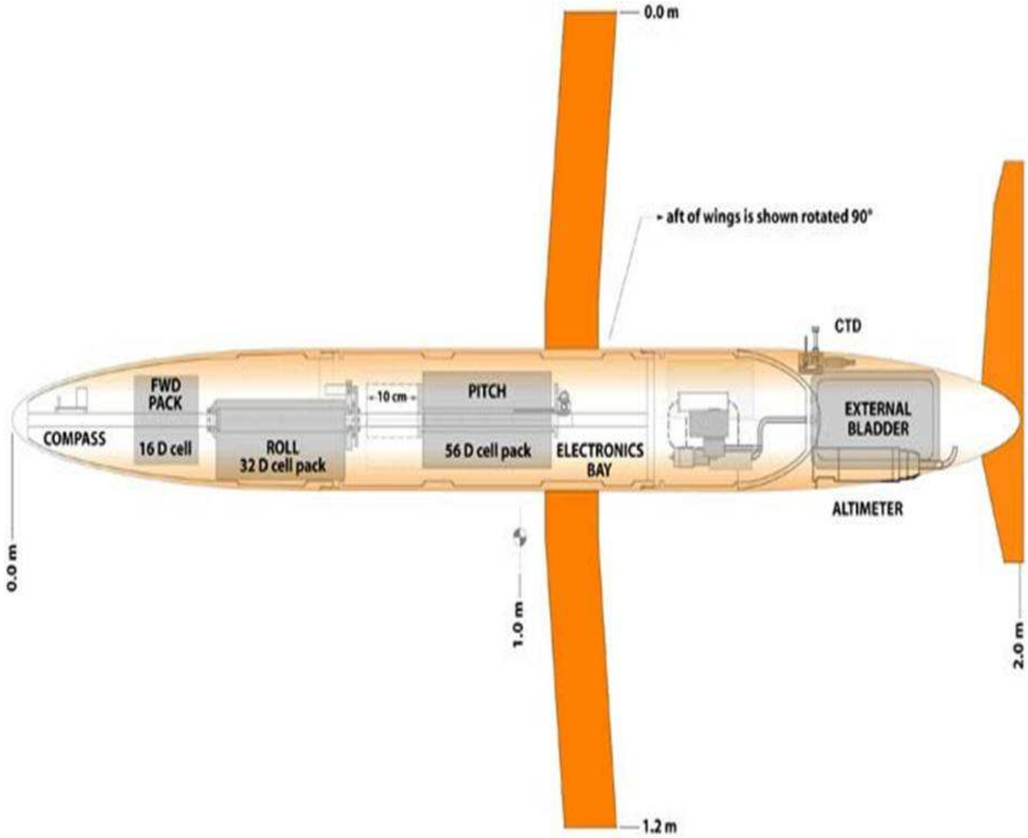

Figure 1.6: Construction of underwater glider.

1.4 Thesis Overview

The goal of this work is to develop a task allocation framework, to select in a localized manner a best possible team of AUVs to accomplish the mission based on work presented in [28, 29]. The fundamental requirement in any mission is the ability to accomplish the required tasks with reliability and in allotted time. The team formed as a result of the task allocation algorithm is the optimal subset of the deployed AUVs that can reliably and efficiently complete the mission. If all the deployed AUVs were selected as a team, the mission may or may not be feasible to accomplish due to the communication overhead and time taken to solve the optimization problem, and even if it were to be accomplished successfully it may be inefficient in terms of resources. Hence, task allocation is required to choose the best possible subset of vehicles in such a way as to reliably accomplish the mission with high time and energy efficiency. For example, missions like rescue of a drowning nuclear powered submarine would require an immediate response from a team of AUVs to find out the location of drowning, to detect any leakage of radioactive substances from it, to temporarily stop the leakage if possible, and to continuously monitor the hazard level of the spillage in order to asses the damage to the marine environment. This is a critical situation as it can cause colossal damage to human life, property and contaminate the marine environment. An optimal response team for such missions based on task allocation for networked AUVs is envisaged in this work.

In Chapter 2, we review the existing work done for communication and coordination of AUVs and terrestrial robots. We also review the work done in the area of underwater acoustic communication. We observe that the work done in the field of control and coordination for AUV teams is very limited. None of the work considers inter AUV communication, which is vital for efficient team coordination and for successful completion of the mission.

In Chapter 3, we propose the task allocation framework, formulation of the optimization problem and an application that involves acoustic imaging of an underwater object. In Sect. 3.1, we describe the basic model assumptions on which the task allocation optimization problem is based on. In Sect. 3.2, we explain in detail time critical networking based on the geocasting protocol. The communication procedure for collecting data and selecting AUVs is described in phases in this section. In Sect. 3.3, we formulate the task allocation optimization problem for gliders, AUVs and a heterogenous team i.e. combined team of AUVs and gliders. In Sect. 3.4, we describe an application for a team of AUVs which involves acquiring acoustic images of an unknown underwater object, by AUVs fitted with side scan sonar.

In Chapter 4, we present the performance evaluation of the simulations performed for task allocation optimization problem and consider various scenarios. In Sect. s4.1, we evaluate the tradeoff between the size of the geocast region and optimality of the solution. In Sect. 4.2, we evaluate the effect of underwater currents on the choice of the geocast region. In Sect. 4.3, we evaluate the localized nature of the problem in absence of underwater currents. In Sect. 4.4, we compare the energy of the team of gliders and PDVs based on the mission length, when the team is deployed for the acoustic imaging mission. In Sect. 4.5, we compare the energy of gliders and PDVs based on the number of vehicles present in the team, when the team is deployed for the acoustic imaging mission.

In Chapter 5, we draw conclusions from the simulation results obtained in chapter 4 and discuss the scope for future work.

Chapter 2

Related Work

In this chapter we review the existing work done in the area of control, coordination and task allocation for AUVs and terrestrial robots. Further, we also review the work done in the area of underwater acoustic communication and various protocols developed specifically for underwater acoustic communication and terrestrial sensor networks. We observe that the work done in the field of control, coordination and task allocation for forming teams of AUVs is very limited. None of the research till date considers inter AUV communication to control, coordinate or perform task allocation for a team of AUV.

While studies have been conducted on communication and coordination of immobile [31] and mobile [32] sensor and actor networks, there has not been any research tailored specific to underwater environment. In [7] the applications of UW-ASNs for ocean exploration and research challenges in design of UW-ASNs consisting of AUVs and fixed sensors are described. It illustrates the use of UW-ASNs in applications like oceanographic data collection, pollution monitoring, offshore exploration, disaster prevention, assisted navigation and tactical surveillance. For effective monitoring of the environment it emphasizes that the AUVs equipped with sensors must posses self configuration capabilities i.e., they must be able to coordinate their operation by exchanging configuration, location and movement information, and to relay monitored data to an onshore station. It highlights the disadvantage of using radio waves and advantage of using acoustic waves for underwater communication. To overcome the disadvantages of deploying stationary sensors like no real time monitoring, no online system reconfiguration, no failure detection, limited storage capacity, UW-ASNs consisting of AUVs are suggested. Authors of [34, 16] propose a control strategy for a group of vehicles to move and reconfigure cooperatively in response to a sensed distributed environment. Each vehicle in the group serves as a mobile sensor and the vehicle network as a mobile and reconfigurable sensor array. The coordination frame work is based upon Virtual Bodies and Artificial Potentials (VBAP). The focus here is on the gradient climbing missions in which mobile sensor network seeks local minima and maxima. The network can adapt its configuration in response to the sensed environment in order to optimize the gradient climb. The virtual body is a collection of linked moving reference points. The vehicle group moves and reconfigures with the virtual body by the means of forces that are derived from artificial potentials between the vehicles and reference points on the virtual body.

Authors of [40] propose a navigation and control strategy for multiple gliders using underwater acoustic communication. They form a underwater communication network by deploying acoustic modems, seafloor mounted sensors and gateway mounted buoys. Underwater gliders are deployed in this network, which act a mobile nodes. Gateway buoys enable underwater nodes to communicate with the vessel using RF communication and base station using satellite communication. The network thus formed is used to control and coordinate a set of gliders to achieve certain objective. The disadvantage of this strategy is that the glider do not intercommunicate and act as team, instead they act a pseudo team in which each glider is individually controlled from the base station or the vessel. Also, the area in which such a technique can be used is limited as it need pre-existing underwater acoustic communication infrastructure.

In [41], the authors study how a team of AUVs can act as a recoverable, reconfigurable array or form a polyhedral structure for monitoring a region of interest in time and space. A model for decentralized control of platoons and emphasize the need for efficient communication among participating AUVs is presented in [12]. Authors propose a coordination framework based on estimation theory and potential distribution for directing the robots to target locations in [13]. We observe that none of the above mentioned work considers the criticality of the mission in the sense of time and reliability; most of the research until date has been, in fact, on passive monitoring and sampling missions. We also observe that no work until date considers PDVs and gliders to form a heterogeneous team.

Extensive research has been done in the area of localization, coordination, and task allocation for terrestrial robots [44, 18, 6, 42], but the work has been very limited for AUVs. In [46], authors propose a decentralized coordination approach based on individual prioritization schemes. In [11], authors propose a probabilistic coordination approach that simultaneously considers cost to reach the target point and utility of the target point. It was observed that coordination algorithms for terrestrial robots are communication intensive, i.e., require large bandwidth, and heavily rely on GPS tracking. Compared to terrestrial environment, underwater the available bandwidth is low, channel is noisy, bit rate is very low, packet loss is high, and GPS tracking is available only at the surface. Hence, AUVs need specially designed algorithms that strictly adhere to the limitations and impairments of underwater acoustic communications.

In [37], the authors propose two energy efficient routing algorithms for delay sensitive and delay insensitive applications in underwater environment. They propose a model that characterizes the acoustic channel utilization efficiency, which helps in investigating some fundamental characteristics of underwater environment. This paper considers a three-dimensional underwater sensor network, but it does not consider mobility of nodes, which is the fundamental requirement of our work. In [35], a reliable and energy efficient scheme for communication in UW-ASNs is proposed. In the protocol proposed in this paper the packet transmission time and energy consumption at the node is reduced compared to standard radio-based broadcast protocols. They give special consideration to the low bandwidth in underwater channels. However, in characterizing the underwater channel the authors have only considered the deterministic transmission losses and neglected the statistical nature of the channel, which is drawback of this protocol. In [45], the authors discuss location aided multicast algorithms in terrestrial sensor networks. They propose three heuristic algorithms: i) Single Branch Regional Flooding (SARF), ii) Single Branch Multicast Tree (SAM), and Cone based Forwarding Area Multicast tree (CoFAM) to construct a multicast tree rooted at source and deliver the packets to nodes in geographic location. None of these algorithms ensure reliable delivery of packets that is necessary for query dissemination in underwater environment. Underwater sensor networks unlike terrestrial sensor networks are sparsely deployed and the query packet needs to be sent to all nodes instead of only a few chosen nodes.

Chapter 3

Proposed Framework

In this chapter, we propose the task allocation framework for the deployed AUVs. We formulate an optimization problem to perform optimal task allocation for the deployed AUVs so as to form the best possible team. The objective of the task allocation framework is to maximize the available energy of the team. The advantage of optimizing the available energy is that after the completion of the mission the AUVs retain enough energy to transmit the data back to the ship overlooking the mission, without surfacing using multi-hop mechanism. This chapter is organized as follows; in Sect. 3.1, we describe the basic model assumptions on which the task allocation optimization problem is based on; in Sect. 3.2, we explain in detail time critical networking based on geocasting protocol; the communication procedure for collecting data and selecting AUVs is described in phases; in Sect. 3.3, we formulate the task allocation optimization problem for gliders, AUVs and a heterogenous team i.e. combined team of AUVs and gliders; in Sect. 3.4, we describe an application for a team of AUVs which involves acquiring acoustic images of an unknown underwater object, by AUVs fitted with side scan sonar.

3.1 Basic Model Assumptions

The task allocation framework proposed in this work is based on certain basic assumptions. The assumptions are as follows:

- It is assumed that the object about which information is to be obtained is present in the region of interest.

- A virtual sphere known as the *object sphere* of radius r [m], as shown in Fig. 3.1, is assumed around the target object.

- A concentric virtual sphere known as *constellation sphere* of radius R [m] is assumed around the object such that $R > r$.

- The radius of the constellation sphere is limited by the maximum distance from which the sensors fitted on the AUVs can acquire data efficiently, which is denoted as R_{max}, note that the minimum distance is the distance that should be maintained between the AUV and the object to avoid collision and damage to sensors.

- All the AUVs in the constellation form a symmetric polyhedral structure known as *constellation polyhedron*, as shown in Fig. 3.1. All the vertices of the polyhedron lie on the constellation sphere such that they are evenly distributed on the surface.

- Each AUV is assigned a unique *optimum position* on the constellation sphere so as to avoid collision between any two AUVs.

- Each AUV is equipped with acoustic modem for underwater wireless communication.

- Each AUV has enough computing power and memory to solve the optimization problem.

- A Mission Observer Ship (MOS), which is capable of collecting and relaying the acquired information to the base station and of communicating with the deployed AUVs using acoustic underwater communication, is assumed to be present near the deployment region or the AUVs are assumed to already have knowledge about the mission and are waiting for an event to occur.

- The base station is assumed to be located far from the region of interest and can communicate only with the MOS via satellite communication.

- Each AUV taking part in the mission knows its approximate distance from the target object.

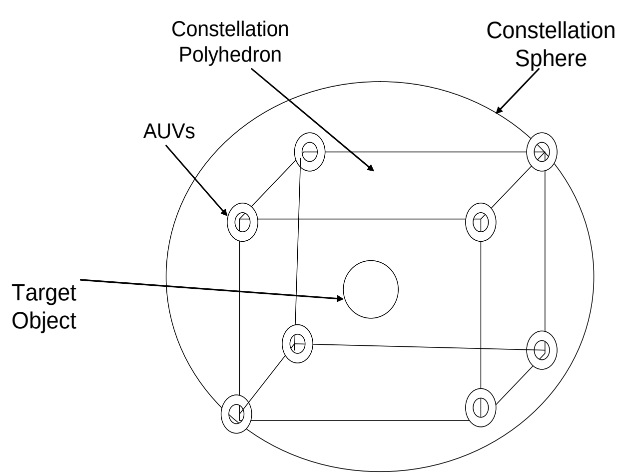

Figure 3.1: Constellation formation to capture object information.

3.2 Time Critical Networking

The success or failure of the mission depends on sharing the time-critical information between the AUVs deployed. The task allocation and team formation process involves sharing of information about the positions of AUVs, ocean currents, available energy, sensors available onboard, type of vehicle, i.e., PDV or glider. This critical information, mandatory to form the team, is shared using underwater acoustic communication.

Formation of an optimal team to accomplish the mission involves five phases:
Phase I involves MOS broadcasting mission details to the AUVs deployed near the target object based on geocasting protocol;
Phase II is the election of a collector AUV from AUVs deployed near the target object based on geocasting of the data;
Phase III consists of finding the AUVs available to be a part of the team;
Phase IV involves solving the optimization problem;
Phase V consists of geocasting the output of the optimization problem in order to inform the AUVs in the geocasting region of their selection as a part of the optimal team;
Phase VI aims at achieving vehicle self-localization via exchange of position information.

The timing diagram for the first five phases is shown in Fig. 3.2. As localization is assumed to be a part of trajectory planning problem, it is not considered in the timing diagram. ***Phase I: Broadcast of mission details to deployed AUVs***
Objective and requirements of the mission are conceived at the base station. The data is relayed to the MOS via satellite communications, as shown in Fig. 3.3. MOS broadcasts the message in the region where the AUVs are deployed, as shown in Fig. 3.3.

The time taken by the broadcast message containing the mission details to reach the AUVs is dependent on the propagation delay T_p[s] and the transmission delay T_r[s] as shown in Fig. 3.2 and is given by,

$$T_p = \frac{d_{sd}}{c}, \tag{3.1}$$

$$T_r = \frac{l_{pkt}}{X_{sd}}, \tag{3.2}$$

where d_{sd} [m] is the distance between the sender and the receiver, c [m/s] is the velocity of sound inside water, l_{pkt} [bits] is the length of the packet, and X_{sd} [kbps] is the transmission

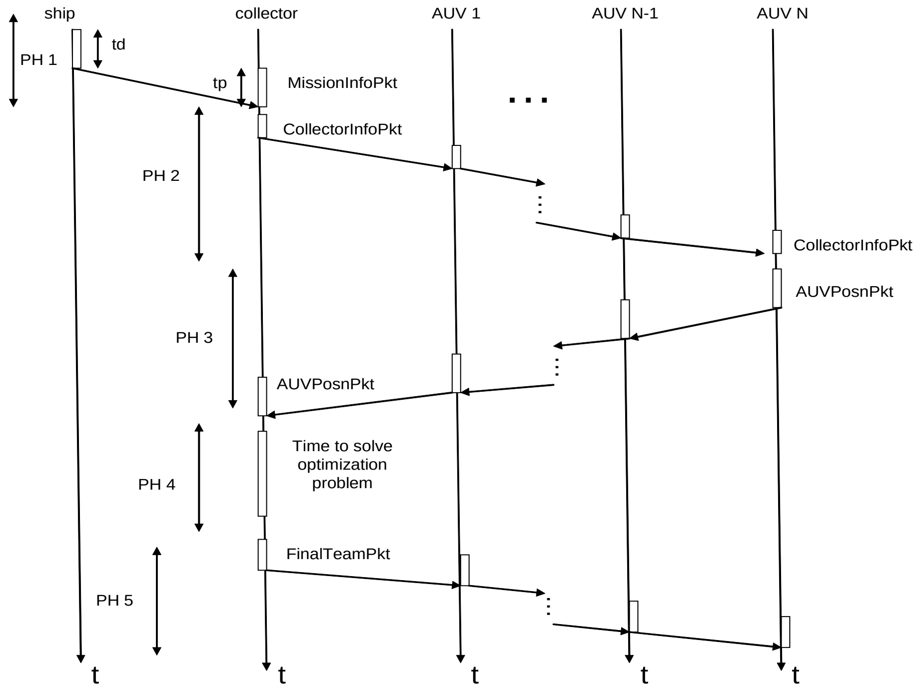

Figure 3.2: Time critical networking for the formation of optimal team of AUVs.

rate. Underwater channel possess unique challenges such as limited bandwidth, severely impaired signal due to multipath and fading, propagation delay that is five orders of magnitude higher than in terrestrial radio frequency communication and variable, high bit error rate and temporary loss of connectivity [7]. Transmission loss in an underwater channel is

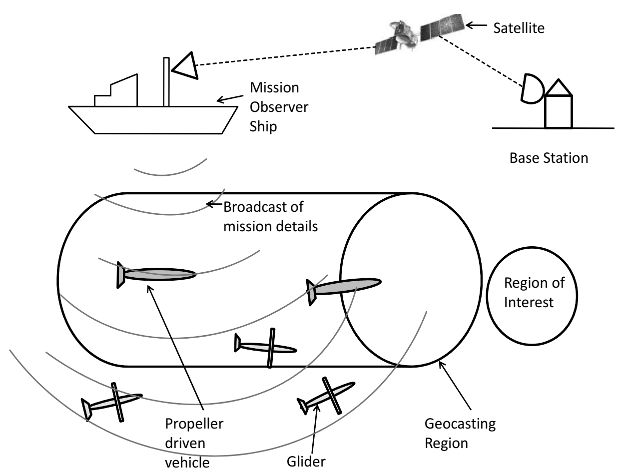

Figure 3.3: Mission Observer Ship (MOS) receiving mission details from the base station via satellite and broadcasting these mission details to the deployed AUVs.

described by the Urick's propagation model [43] and is given by,

$$TL^D(d, f_o) = 20 \cdot \log(d) + \beta(f_o) \cdot d, \tag{3.3}$$

where $TL^D(d, f_o)$ [dB] is the deterministic transmission loss of a narrow band acoustic signal with a center frequency of f_o [kHz] experienced along a distance d [m] and $\beta(f_o)$ [dB/m] represents the medium absorption coefficient and quantifies the dependency of transmission loss on frequency band. The statistical transmission loss model of the channel is developed in [8]. To model the statistical loss the water body where the AUVs are deployed is assumed to be a parallelepiped and is divided into cubes w, h, etc., each with side S_c $[m]$, which is taken as coherence distance. A matrix $\Psi(t_k) = [\gamma_{wh}]$ is formed, such that it stores the value of random variable γ with unit-mean Rayleigh distribution, to account for statistical attenuation in the channel from cube w and h. The statistical attenuation is given by,

$$TL_{ij}(t_k) = TL_{ij}^D \cdot \gamma_{wh}^2, \tag{3.4}$$

where i and j are sending and receiving AUVs respectively, w and h are the cubes where i and j are located respectively, while γ is an element in the matrix Ψ at time t_k that is recomputed every T_c [s], which is the coherence time of the channel. Special properties of matrix Ψ are: i) $\gamma_{ww} = 1$ (transmission loss within the coherence distance), ii) $\gamma_{wh} \neq \gamma_{hw}$, i.e., link asymmetry, iii) Ψ is memory less, i.e., $\Psi(t_{k+1})$ does not depend on $\Psi(t_k)$. This model takes into consideration the spatio-temporal variation and link asymmetry, which are peculiar characteristics of the underwater acoustic channel, and accounts for the worst-case scenario where the channel is in 'saturated conditions', i.e., it is affected by heavy multipath (e.g., in shallow water).

Phase II: Election of the collector

A collector AUV, selected from the deployed set, collects the information from all the other deployed AUVs and solves the optimization problem to select the best possible team for the mission. Once an AUV receives the mission details from the MOS, it starts a *hold-off* timer, after the end of which it will broadcast a message to inform all the other AUVs deployed in the region of its role as a collector, as shown in Fig. 3.3. The collector election is implemented based on the geocasting mechanism. The collector AUV then aims at reaching maximum number of AUVs; ideally all the AUVs deployed in the region so as to form the best possible team. To achieve this there is a necessity to de-synchronize the transmission from different AUVs to avoid collisions of packets. If an AUV receives a packet it decides not to further transmit and is thus out of competition for being a collector. To achieve de-synchronization each AUV starts a *hold-off* timer. The *hold-off* timer, T_{hold} [s], is a uniform random variable in $[0, 2T_{hold}^{mean}]$, where T_{hold}^{mean} is given as,

$$T_{hold}^{mean} = \frac{d_{io}}{d_{so}} \cdot \tau + \frac{\Phi_{si}}{v_{sound}} + t_d, \tag{3.5}$$

$$\Phi_{si} = \begin{cases} R_{max} - d_{si} & \text{if } R_{max} \geq d_{si} \\ 0 & \text{if } R_{max} < d_{si} \end{cases}$$

where d_{si} [m] is the distance between the sender AUV, 's' and receiver AUV 'i', d_{id} is the distance between the AUV 'i' and the target object 'o', d_{so} is the distance between the sender AUV and the target object, τ [s] is a constant, $\frac{\Phi_{si}}{v_{sound}}$ [s] is the propagation delay equivalent to t_p [s] in (3.1), t_d is the transmission delay given by (3.2), R_{max} [m] is the maximum distance from which the AUV can acquire the object information effectively and depends on the type of sensor mounted on it. The transmission rate X_{sd} in (3.2) is given by

$$X_{sd} = \eta \cdot \frac{C_{ch}}{N_{reg}}, \tag{3.6}$$

where C_{ch} [kbps] is the capacity of the channel and N_{reg} is the number of AUVs present in the geocasting region, η is a constant, when $\eta = 1$ the channel is ideal. For practical purposes $\eta < 1$.

The mean value of the hold-off timer T_{hold}^{mean} in (3.5) is chosen such that it de-synchronizes a AUVs transmission from its neighbors transmission and avoids collision at the receiver. The factor $\frac{d_{io}}{d_{so}} \cdot \tau$, de-synchronizes the transmission of the AUVs. Closer the AUV to the destination, smaller is the hold-off timer. The factor $\frac{\Phi_{si}}{c} + t_r$, adds the extra propagation and transmission delay to receive the packet at destination. If two AUVs 'i' and 'j' have equal distance from the sender and target object, i.e. $d_{io} = d_{jo}$ and $d_{si} = d_{sj}$. Such AUVs have equal value of T_{hold}^{mean}, which makes necessary the use of random hold-off timers in order to de-synchronize the transmissions from AUVs 'i' and 'j'. During the hold-off period if an AUV overhears a packet it stops the hold-off timer and elects itself out of the competition for being the collector.

Phase III: Selection of available set of AUVs using geocasting protocol

The AUVs selected in this phase using the geocasting protocol act as input to the optimization problem. The collector once elected starts collecting information required to solve the optimization problem. For collecting information it uses a geocasting mechanism as underwater acoustic communication is slow and less reliable as compared to the terrestrial radio frequency communication. Reliability is the primary concern in underwater acoustic communication. In multi hop networks reliability can be provided on an end-to-end or on a hop-by-hop basis. Whereas end-to-end reliability ensures successful transmission between source and destination, hop-by-hop reliability ensures successful transmission between a pair of nodes. End-to-end approach does not hold good for underwater networks due to the high channel error probability and the low propagation speed of acoustic signals because; 1) the high channel error probability makes the probability of successfully transferring data from end to end almost approaching to zero, as this results in too many retransmissions for a successful packet delivery; 2) the low propagation speed of acoustic signals 1500 [m/s] will cause very large end-to-end delay, which introduces difficulty for the two ends to manage data transmission in a timely manner. For these reasons we rely on link layer mechanisms to provide hop-by-hop reliability. Specifically, we aim at maximizing the end-to-end reliability by providing high link layer reliability. We propose a reliable geocasting protocol which integrates the MAC and routing layer functionalities but assumes no neighbor knowledge.

Geocasting in wireless sensor networks and adhoc networks is the delivery of a message from a source to all the nodes in a geographical region [25, 26]. Dissemination of query inside the geographical region is defined by the sender. Geocasting can be easily achieved by flooding the network thereby reaching all the nodes in the geocast region. In geocasting protocol, we leverage the shape of the geocast region using the information included in the transmitted query packet. Assuming the geocast region to be cylindrical, the surface station includes the following information about the geocast region in the query packet: the geographical co-ordinates of the center 'C_g' of the geocast region, vector $\overrightarrow{L}$ along the longest side of the geocast region and passing through the center, radius 'r_g' of the cylindrical region as shown in Fig. 3.4. If $\overrightarrow{si}$ is the vector from the sender 's' to the receiver 'i' of the query packet, the projection of the vector $\overrightarrow{si}$ along vector $\overrightarrow{v}$ is given by,

$$d_{si} = \overrightarrow{si} \cdot \frac{\overrightarrow{L}}{\|\overrightarrow{L}\|} \tag{3.7}$$

A node receiving the query packet determines if it lies in the geocast region, with the help of the above information transmitted in the query packet, and knowledge of its own geographical location. Every node lying inside the geocast region and receiving the packet follows the protocol for query dissemination inside the region. If a node lying outside the geocast region receives a packet, it discards it.

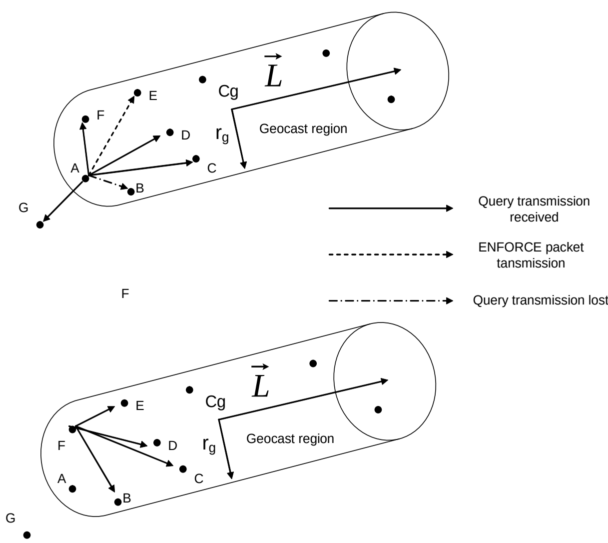

Figure 3.4: Broadcast in the geocast region

Consider the shape of geocast region as shown in the Fig. 3.4. Let us say the query packet enters the geocast region through the node A. Node A then broadcasts a short ENFORCE packet. Immediately after broadcasting the ENFORCE packet, node A transmits the query packet. The ENFORCE packet alerts the nodes that a query packet is to be expected after a certain interval of time, due to this the nodes who want to transmit data defer their transmissions accordingly. Also as the ENFORCE packet is short, the transmit time, receive time and hence the probability of packet collision is less. On receiving the query packet for the first time, the nodes E, D, C and B start a hold-off timer, $T_{hold}^{geocast}$. $T_{hold}^{geocast}$ is a uniform random variable in $[0, 2T_{hold-mean}^{geocast}]$ where $T_{hold-mean}^{geocast}$ is given by,

$$T_{hold-mean}^{geocast} = (1 - \frac{d_{si}}{R_max} \cdot \tau + \frac{\phi_{si}}{v_{sound}}), \tag{3.8}$$

$$\Phi_{si} = \begin{cases} R_{max} - d_{si} & \text{if } R_{max} \geq d_{si} \\ 0 & \text{if } R_{max} < d_{si} \end{cases}$$

where d_{si} is the projection of the vector $\overrightarrow{si}$ along the vector $\overrightarrow{v}$ passing through 's'. The idea is to give higher priority to nodes having a greater value of d_{si} so that the query packet quickly penetrates the length of the geocast region. From the Fig. 3.4, one can see that node C will have the smallest hold-off timer as compared to other receiving nodes. Once node C's hold-off timer expires, it broadcasts the packet. A node while still being in the hold off state, will wait to overhear transmissions from all directions except from the sender's direction. The node that fails to overhear from any one of these directions will decide to be a forwarding node. A non-forwarding node simply stops its hold-off timer whereas forwarding node broadcasts the packet once the hold-off timer expires.

A node that does not receive the query packet but receives the ENFORCE packet decides to inform other nodes that it did not receive the query packet by sending a NACK. Before transmitting a NACK, the node waits for a duration of NACK-hold-off timer given by,

$$T^{geocast}_{NACK-hold-off} = T^{geocast}_{hold-max} + \frac{R_{max}}{v_{sound}} + t^{Q}_{d}, \tag{3.9}$$

where t^{Q}_{d} is the transmission delay for the NACK.

In the Fig. 3.4, it can be seen that node F will transmit a NACK. The NACK hold-off timer ensures that F waits long enough to overhear the transmission from a forwarding node in the neighborhood if any. If F is not able to overhear before NACK-hold off timer expires, it will transmit the NACK and start a NACK-timeout timer given by,

$$T_{NACK-timeout} = 2\frac{R_{max}}{v_{sound}} + t^{Q}_{d} \tag{3.10}$$

A node that receives the NACK will respond with probability $P(N) = \frac{n}{n+2}$ where n is the number of NACK's received. A node that receives the highest number of NACKs will have a higher probability to respond. If a node does not get the packet during NACK timeout period, it will retransmit the NACK.

The Finite State machine (FSM) for a node with no neighbor knowledge is as shown in

Fig. 3.5. A node has five states: 'idle', 'wait', 'transmitted query', 'transmitted ENFORCE' and 'NACK received' state. On receiving a NACK, a node enters 'NACK received' state and goes back to 'idle' state if it statistically decides not to transmit the query. A node is in 'wait' state when either of its timers are active. When hold-off timer for ENFORCE expires, a node enters 'transmitted ENFORCE', transmits ENFORCE and then enters 'transmitted query' state. Consequently, it transmits the query packet and enters an 'idle' state. This

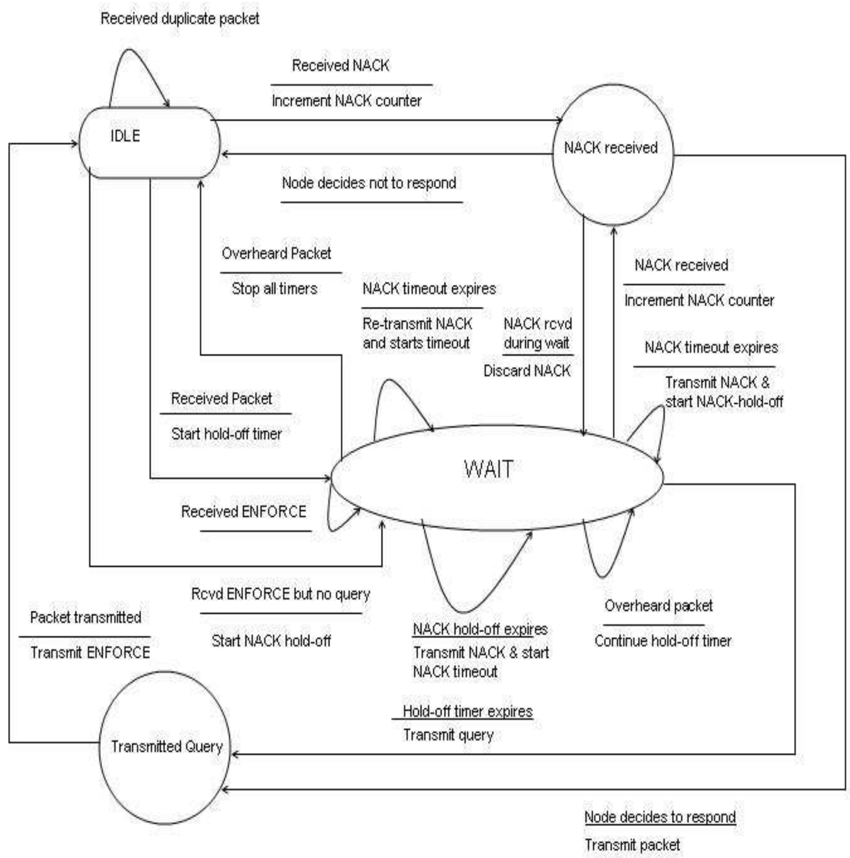

Figure 3.5: Finite State Machine (FSM) for a node inside the geocast region with no neighbor knowledge

geocasting protocol is used by the collector AUV to acquire data from the other AUVs deployed in the geocast region. The center of the geocast region is same as the center of the target object when underwater currents are not considered. In the presence of underwater currents the geocast region can be shifted in the direction opposite to direction of current so as to include maximum number of AUVs traveling in the direction of current in the optimization problem, which may lead to more optimal solution. If one or two hop neighbor knowledge is considered the time for data collection at collector can be reduced drastically and it is left for future research to find out the optimality of the protocol assuming one or two hop neighbor knowledge.

Phase IV: Solving the task optimization problem

The optimization problem formulated in Sect. 3.3, is solved by the collector AUV. The optimization problem chooses the best possible set of networked AUVs to accomplish the mission. As the optimization problem is substantially complex and involves many variables, the time to solve it depends on the processing power of the AUV. The computing power available on the AUV is limited as it is shared for controlling the AUV, processing sensor information, and solving the optimization problem. Hence, it may take more time to solve the problem than on a computer dedicated for such a task.

Phase V: Geocasting mission details

After the optimization problem is solved the AUVs selected as a part of the team are informed about their mission details. The mission details are geocasted by the collector AUV. If the AUV that is not selected in the team receives the message it discards it.

Phase VI: Localization

Once selected in the team, the AUVs localize themselves with respect to the rest of the team. A simple localization approach based on dead reckoning and acoustic communication is used in this work. Dead reckoning is a navigation system that uses readings from compass, depth sensor, and speed sensor together to calculate the current position with respect to the initial position where GPS information was available. It is prone to error due to the drift caused by underwater currents and it adds cumulatively with time. To improve the accuracy of dead reckoning we propose a simple geocasting-based feedback mechanism. The AUV geocasts a query asking for the coordinates of the adjacent AUVs selected as a part of the team. Response from at least one neighbor is required for team size greater than one. Based on the response time and velocity of sound in water, the broadcasting AUV knows its distance from the responding AUV. Broadcasting AUV uses this distance and coordinates of the responding AUV obtained in the response to the query to find its coordinates using standard Euclidean distance. The broadcasting AUV compares this position with its dead reckoning system reading and computes the error, which is fed back to dead reckoning calculator to increase its accuracy. Advanced localization algorithms are proposed in [20, 10].

Note that the time taken to implement Phase I to Phase V reduces the *actual time* available for the mission. Hence, selecting a large geocasting region is not always a good choice as more time may be spent on communication and solving the task allocation problem, which may make accomplishing the mission impossible in the allotted time.

3.3 Problem Formulation

In this section we formulate the mathematical models for the formation of the optimal team to accomplish the given mission. The objective function has the aim to either *optimize energy* or to *optimize time* depending on the mission requirements. The objective function for *optimizing energy* has three subcategories: i) maximize the available energy of the team of AUVs after the mission; ii) minimize the energy required by the team of AUVs to complete the mission; and iii) maximize the minimum available energy of AUV that is part of the team, which in turn maximizes the life time of the team, while respecting the time bound δ [s] for the mission. Conversely, the objective function to *optimize time* aims at minimizing the time required to complete the entire mission even at the cost of a higher energy expenditure. In this section, we first formulate the optimization problem for only gliders, then for only PDVs, and finally for both PDVs and gliders together (heterogenous team). The optimization problem proposed in this work is focused on maximizing the available energy of the team after the completion of mission as the energy saved can be used to transmit the data collected from the target object to the MOS.

3.3.1 Effect of Underwater Currents on Optimization Problem

Underwater currents are caused due to small streams and rivulets inside the water body. Due to underwater currents the solution of the optimization problem is affected drastically. The problem, in fact, cannot be considered localized in the presence of underwater currents. Underwater currents can make involving an AUV that is aligned with the direction of current but far from the target object beneficial; conversely, an AUV close to target object but facing opposite to current may not be the best choice to be a part of the team. The drift would push the AUV aligned with the current forward, and it would need same or lower energy to travel at an increased speed. In contrast, an AUV traveling opposite to the current has to spend more energy to overcome the force of current, even to travel at its normal speed. It is assumed that under ideal case ocean current does not change with depth and are present only in the horizontal plane [38]. The force $\overrightarrow{F}_c$ acting on an AUV due to underwater current is given as,

$$\overrightarrow{F}_c = C_c \sigma A_{AUV} \cdot (\overrightarrow{V}_c - \overrightarrow{V}_{AUV}), \tag{3.11}$$

where $\overrightarrow{V_c}$ [m/s] is the horizontal velocity of underwater current, $\overrightarrow{V}_{AUV}$ [m/s] is the horizontal velocity of the AUV, A_{AUV} [m^2] is the cross-sectional area of the AUV, σ is a constant dependent on the shape of the AUV through $C_c = 721.1$ [Ns/m^3] (C_c is the resistance due to momentum of the AUV).

3.3.2 Buoyancy-driven Gliders

In this section we consider that the AUVs deployed are only gliders. The optimization problem is formulated to maximize the available energy for the team of gliders. Based on the assumptions in Sect. 3.1, the aim is to find the optimal number of gliders to form a team based on the objective function to accomplish the mission respecting the time bound δ [s].

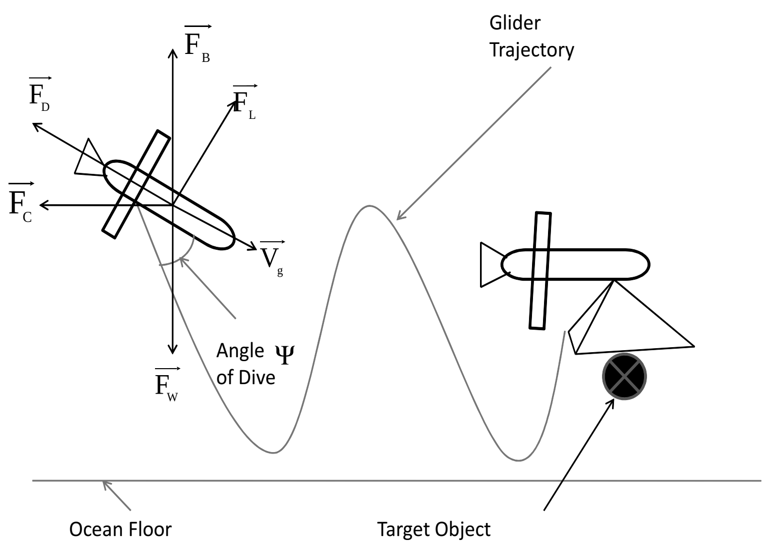

Figure 3.6: Sawtooth trajectory of the glider.

We also analyze the dynamics of the glider and evaluate the effect of ocean currents on the task optimization problem. From Sec. 3.3.1, it is assumed that under ideal case ocean currents do not change with depth [38], and gliders move in a sawtooth trajectory as sketched in Fig. 3.6. The forces acting on the glider, as shown in Fig. 3.6, are

$$\vec{F}_{total} = \vec{F}_w + \vec{F}_b + \vec{F}_c + \vec{F}_{drag} + \vec{F}_{lift}, \tag{3.12}$$

where $\vec{F}_w = \rho_{glider} vol_{glider} \cdot \vec{g}$ is the weight force, which depends on the density ρ_{glider} [kg/m^3] and volume vol_{glider} [m^3] of the glider and on the terrestrial gravitation g [m/s^2][19]. $\vec{F}_b = \rho_{water} vol_{glider} \cdot \vec{g}$ is the buoyant force due to Archimedes' principle, which is equal to the weight of the displaced fluid by the glider, where $\rho_{water} = 1050$ [kg/m^3] represents the average density of salty water, $\vec{F}_c = C\sigma A_g \cdot (\vec{V}_c - \vec{V}_g)$ is the force of current as defined in (3.11), $\vec{V}_g$ is the horizontal velocity of the glider and A_g is the cross sectional area of the glider, $\vec{F}_{drag} = \frac{1}{2}\rho_{water} C_{drag}(\theta) A_g \cdot \vec{V}_g^2$ is the drag force, and $\vec{F}_{lift} = \frac{1}{2}\rho_{water} C_{lift}(\theta) A_g \cdot \vec{V}_g^2$ is the lift force; these forces are proportional to the square of velocity of the glider $\vec{V}_g$ [m/s], cross-sectional area of the glider A_g [m^2], and the density of the salty water through the constants C_{drag} and C_{lift}, respectively, which are dependent on the angle of dive θ.

The power required to move the glider is equivalent to the product of force required to counterbalance the force in (3.12) and move at velocity V_g. The glider moves in a sawtooth trajectory, which is unique as compared to other underwater vehicles. This has the advantage of conserving engine power as it needs energy only to climb, but it makes the model very complicated. Glider requires more power to climb as compared to dive, as it has to pump out water with a force equivalent to $\vec{F}_{total}$ to travel at velocity V_g. Hence, in the mathematical model we consider only the power required to climb. It is assumed for simplicity that the glider dives at a constant angle, hence, the horizontal distance covered in one dive or climb can be calculated as,

$$dist_{cov} = \tan(\theta) \cdot (depth_{fl} - depth_{gl}), \tag{3.13}$$

where $dist_{cov}$ is the horizontal distance covered by the glider diving at an angle θ and is present at depth $depth_{gl}$ with respect to the surface, and $depth_{fl}$ is the average depth of the sea floor in the given region with respect to the surface. It is assumed that the glider starts and ends the mission with a dive. Depending on the horizontal distance the glider is required to cover, the number of dives and climbs can be calculated as,

$$N_{climbs} = \frac{1}{2}\frac{dist_{trav}}{dist_{cov}}, \tag{3.14}$$

where N_{climbs} is the number of times the glider climbs in traveling a total distance of $dist_{trav}$ [km]. The glider engine is on for the time T_{pump} required to pump out the water, which is of the order of minutes. From N_{climbs}, the number of times the glider climbs is known and, hence, the total time for which the engine is 'on' can be calculated as,

$$T_{on} = N_{climbs} \cdot T_{pump}, \tag{3.15}$$

where T_{on} is the total time for which the pump operates during the mission and T_{pump} is the time the pump needs to be on for one climb at velocity V_g.

In the following, for the sake of clarity, we introduce the notations for construction of our mathematical model for gliders:

- $Pos^i_g(x^i_g, y^i_g, z^i_g)$ is the *initial position* of glider g in the deployment region, $Pos^f_g(x^f_g, y^f_g, z^f_g)$ is the optimum position f on the *constellation sphere* of the glider g around the target object, $C_o(x_o, y_o, z_o)$ is the center of the *object sphere* with radius r and Z_{fl} [km] is the depth of the ocean floor from the surface assuming the sea bed to be uniform.
- P^M [W] is the power required to run the buoyancy engine.
- $\mathcal{G}$ is the set of gliders deployed in the region; every glider g is its element and X_g is a binary vector determining which gliders are selected in the team for the mission.
- T^M_g [hr] is the time glider g requires to move a certain distance at horizontal velocity V^{eff}_g [km/hr].
- T^Ω_g [hr] is the time required to collect data from the target object by the respective glider.
- T_{on} [hr] is the time for which the buoyancy engine is 'on' and it is determined by the velocity V_g of the glider.
- T_{pump} [hr] is the time for which the buoyancy engine is 'on' for one climb and T^{Total} [hr] is the time the team of gliders will take to complete the mission.
- E^M_g [J] is the energy required by the glider g to move from initial position to the optimum position.
- E^Ω_g [J] is the energy required by the glider to move around the target object to acquire data.

- E_g^{Av} [J] is the energy available to the glider before the start of the mission.
- δ [hr] is the total time bound to complete the mission.
- α [degrees] is the angle that a glider makes with the direction of underwater current.
- T_{comm} is the sum of the time required for communication from Phase I to Phase V. Phase I to Phase IV are completed before solving the optimization problem, hence the time utilized by them is already known. For Phase V, the time is assumed to be same as time required for Phase III.

Now, we introduce a specific framework that presents a mathematical model that takes into consideration the initial position of the deployed gliders, optimum position of the gliders in the constellation, size of the object, time bound for the mission, energy of the gliders participating in optimization problem before the start of mission, and the angle made by each participating glider with the direction of ocean current. The velocity of gliders has a very limited range of variation as compared to that of PDVs; hence, in this mathematical model we assume the velocity of all gliders to be constant.

The problem is formulated as a *Mixed Integer Non Linear Program (MINLP)*. The objective of the problem is to maximize the available energy after the completion of the mission while respecting the time bound δ.

Multi-glider Task Optimization Problem

$$
\begin{aligned}
\textbf{Given}: &\quad Pos_g^i, C_o, \mathcal{G}, P_g^M, R_{min}, R_{max}, \\
&\quad \delta, V_g, T_{on}, F_{total}, \alpha, E_g^{AV}, T_{pump}, V_c, T_{comm} \\
\textbf{Find}: &\quad Pos_g^{f*}, X_g^*, R^* \epsilon [R_{min}, R_{max}] \\
\textbf{Maximize}: &\quad \textstyle\sum_{g\epsilon\mathcal{G}} [E_g^{AV} - (E_g^M + E_g^{\Omega})] \cdot X_g \\
\textbf{Subject to}: &
\end{aligned}
$$

$$E_g^M = P_g^M \cdot T_{on}^M; \tag{3.16}$$

$$P_g^M = F_{total} \cdot V_g^{eff}; \tag{3.17}$$

$$V_g^{eff} = |V_g \cdot cos(\alpha)| + |V_c|; \tag{3.18}$$

$$T_{on}^M = \frac{\sqrt{(x_g^f - x_o)^2 + (y_g^f - y_o)^2}}{\tan(\theta)(z_{fl} - z_o)} \cdot T_{pump}; \tag{3.19}$$

$$T_g^M = \frac{\sqrt{(x_g^f - x_o)^2 + (y_g^f - y_o)^2}}{V_g^{eff}}; \tag{3.20}$$

$$E_g^{\Omega} = P_g^{\Omega} \cdot T_{on}^{\Omega}; \tag{3.21}$$

$$T_{on}^{\Omega} = \frac{2 \cdot \pi \cdot R}{\tan(\theta)(z_{total} - z_o)} \cdot T_{pump}; \tag{3.22}$$

$$T_g^{\Omega} = \frac{2 \cdot \pi \cdot R}{V_g^{eff}}; \tag{3.23}$$

$$T^{Total} = \frac{1 + \sum_{g=1}^{|\mathcal{G}|} (\frac{T_g^M}{T_g^{\Omega}}) \cdot X_g}{\sum_{g=1}^{|\mathcal{G}|} \frac{X_g}{T_g^{\Omega}}} \leq \delta - T_{comm}; \tag{3.24}$$

$$[(x_g^f - x_o)^2 + (y_g^f - y_o)^2 + (z_g^f - z_o)^2] \cdot X_g = R^2; \tag{3.25}$$

$$\sum_{g\epsilon\mathcal{G}} X_g \geq 1; \tag{3.26}$$

$$\sum_{g\epsilon\mathcal{G}} X_g \leq |\mathcal{G}|. \tag{3.27}$$

Eq. (3.16) determines the energy the glider requires to operate its buoyancy engine while pumping out the water and to travel at a horizontal velocity V_g^{eff}, where V_g is assumed to be constant as it does not vary over a wide range as compared to AUVs. Eq. (3.17) determines the power required to operate the buoyancy engine and to generate a total force equivalent to F_{total} so as to maintain a horizontal velocity V_g^{eff}. Eq. (3.18) determines the effective horizontal velocity of the glider V_g^{eff} when the glider makes an angle α with the direction of underwater current. Constraint (3.19) determines the total time for which the buoyancy engine will operate when the glider moves from its initial position to its optimum position. This is calculated as a product of N_{climbs} and T_{pump}. Eq. (3.20) determines the time required by the glider to travel from its initial position to its optimum position at velocity V_g^{eff}. Eq. (3.21), determines the energy that the glider requires to move when it is acquiring the data from the target object. As the energy to operate the sensors and collect data is small compared to the energy to move, the dominant energy to move around the object is considered. Eq. (3.22) determines the total time for which the buoyancy engine will be on during the data acquisition from the target object. Eq. (3.23) determines the total time required to acquire the data from the object by a single glider; this is the time the glider would need to acquire the data as it will hop from one *optimal position* to another on the *constellation polyhedron*. Constraint (3.24) determines the total time the team of gliders will take to complete the mission and assures that this time be less than or equal to the given time bound $(\delta - T_{comm})$; this is a very important constraint as it is a modification of the assumption that all gliders start scanning the object simultaneously. In this task allocation framework, we consider that if a glider arrives at the object it will start acquiring data - even before the other gliders in the team arrive; hence, the actual work to be done for the joining gliders is less than what they would have shared if all of them would have arrived simultaneously. This constraint is the backbone for critical missions as it ensures that even if the focus is on minimizing the available energy there will be no compromise on time to complete the mission. For derivation of constraint (3.24), see the appendix. Constraint (3.25) puts bounds on the distance between the center of the *object sphere* and the *optimal position* of the gliders selected in the team such that all gliders position themselves on the *constellation sphere*. Constraint (3.26) assures that at least one gliders is always selected to form a team for the mission. Constraint (3.27) assures that the total number of gliders selected for the mission does not exceed the cardinality of the set $\mathcal{G}$.

3.3.3 Propeller-driven AUVs (PDVs)

There is a fundamental difference in the operation of PDVs and gliders. While gliders travel in sawtooth trajectory, there is no constraint on the trajectory of PDVs, i.e., they can travel in straight line, circular path, or a sawtooth trajectory. PDVs are capable of changing their velocity over a broad range but at the cost of some extra energy; hence, they are considered in this work to have variable velocity. The sum of forces $\overrightarrow{F}_{total}$ acting on the PDV are same as those acting on a glider, as given in (3.12).

We introduce the following notation for construction of our PDV specific mathematical model:

- $Pos_p^i(x_p^i, y_p^i, z_p^i)$ is the *initial position* of PDV p in the deployment region, $Pos_p^f(x_p^f, y_p^f, z_p^f)$ is the optimum position f on the *constellation sphere* of the PDV p around the target object, $C_o(x_o, y_o, z_o)$ is the center of the *object sphere* with radius r [m] and $Z = |(z_p^f - z_p^i)|$ [km] is the depth that PDV needs to achieve.
- P_p^M [W] is the power required to run the propeller engine.
- $\mathcal{A}$ is the set of PDVs deployed in the region and every PDV p is its element and X_p is a binary set determining, which PDVs are selected in the team for the mission.
- T_p^M [hr] is the time PDV p requires to move a certain distance at horizontal velocity V_p [km/hr].
- T_p^Ω [hr] is the time required to scan the target object by the respective PDV and T^{Total} [hr] is the time the team of PDVs will take to complete the mission.
- E_p^M [J] is the energy required by the PDV p to move from initial position to the optimum position.
- E_p^Ω [J] is the energy required by the PDV to move around the object to acquire all the data.
- E_p^{Av} is the energy available to the PDV before the start of the mission.
- δ [hr] is the total time allotted to complete the mission.
- α [degrees] is the angle the PDV make with the direction of the ocean current.
- T_{comm} is the sum of the time required for communication from Phase I to Phase V. Phase I to Phase IV are completed before solving the optimization problem, hence the time utilized by them is already known. For Phase V the time is assumed to be same as time required for Phase III.

The objective of the optimization problem is to maximize the available energy of the PDVs after the completion of the mission.

Multi-PDV Task Optimization Problem

$$\begin{aligned}
\textbf{Given}: &\quad Pos_p^i, C_o, \mathcal{A}, r, P_p^M, R_{min}, R_{max},\\
&\quad \delta, V_p, F_{total}, E_p^{AV}, \alpha, V_c, T_{comm}\\
\textbf{Find}: &\quad Pos_p^{f*}, X_p^*, R^* \epsilon [R_{min}, R_{max}]\\
\textbf{Maximize}: &\quad \textstyle\sum_{p\epsilon\mathcal{A}} [E_p^{AV} - (E_p^M + E_p^{\Omega})] \cdot X_p\\
\textbf{Subject to}: &
\end{aligned} \tag{3.28}$$

$$E_p^M = P_p^M \cdot T_p^M; \tag{3.29}$$

$$P_p^M = [\zeta F_{total} \cdot V_p^{eff} + P_{min}^M]; \tag{3.30}$$

$$V_p^{eff} = |V_p \cdot cos(\alpha)| + |V_c|; \tag{3.31}$$

$$T_p^M = \frac{\sqrt{(x_p^f - x_o)^2 + (y_p^f - y_o)^2}}{V_p^{eff}}; \tag{3.32}$$

$$E_p^{\Omega} = P^M \cdot T_p^{\Omega}; \tag{3.33}$$

$$T_p^{\Omega} = \frac{2 \cdot \pi \cdot R}{V_p^{eff}}; \tag{3.34}$$

$$T^{Total} = \frac{1 + \sum_{p=1}^{|\mathcal{A}|} (\frac{T_p^M}{T_p^{\Omega}}) \cdot X_p}{\sum_{p=1}^{|\mathcal{A}|} \frac{X_p}{T_p^{\Omega}}} \leq (\delta - T_{comm}); \tag{3.35}$$

$$[(x_p^f - x_o)^2 + (y_p^f - y_o)^2 + (z_p^f - z_o)^2] \cdot X_p = R^2; \tag{3.36}$$

$$\sum_{a\epsilon\mathcal{A}} X_p \geq 1; \tag{3.37}$$

$$\sum_{a\epsilon\mathcal{A}} X_p \leq |\mathcal{A}|. \tag{3.38}$$

Eq. (3.29) determines the total energy to move the PDV from its initial position to it optimum position on the *constellation sphere*. Eq. (3.30) determines the power required for a PDV to propel itself. Unlike gliders, PDVs require their propellers to be on for the full length of the mission. The power consists of two terms, P^M_{min} [W], which is the power required by the onboard electronics and the propeller control system, and $\zeta F_{total} \cdot V_p^{eff}$ [W], which is a nonlinear term that varies according to velocity V_p^{eff} of the PDV. Eq. (3.31) determines the effective velocity of the PDV. Eq. (3.32) determines the time required to travel from initial to the optimal position at velocity V_p^{eff}. Eq. (3.33) determines the total energy required by the PDV to move around the object on the surface of the *constellation sphere* while acquiring the data. The energy to move is much larger as compared to the energy to acquire data, hence the more dominant energy to move is considered. Eq. (3.34) determines the time the PDV will take to scan the complete object alone. Constraint (3.35) determines the total time the team of PDVs will take to complete the mission and assures that this time be less than or equal to the given time bound $(\delta - T_{comm})$. This is same as constraint 3.24 and its derivation is given in the appendix. Constraint (3.36) puts bounds on the distance between center of the *object sphere* and the *optimum position* of the PDV selected in the team such that all PDVs lie on the *constellation sphere*. It assures that all the PDVs be placed on the constellation sphere. Constraint (3.37) assures that at least one PDV is always selected for the mission to form a team. Constraint (3.38) assures that the total number of PDVs selected for the mission do not exceed the available set $\mathcal{A}$.

3.3.4 Heterogenous Set of Vehicles (Gliders and PDVs)

In this section we assume that the deployed set of AUVs consist of PDVs and gliders. This makes the optimization problem more complex as the energy consumed by gliders is less than that of PDVs; on the other hand, PDVs can move faster than gliders. There is a speed/energy tradeoff between PDVs and gliders, respectively. The notation and mathematical models have been already introduced for the gliders in Sect. 3.3.2 and in Sect. 3.3.3 for PDVs.

For heterogenous deployment, the constraints that change are the total time for the mission, the minimum size, and the maximum size of the team given by,

$$T^{Total} = \frac{1 + [\sum_{g=1}^{|\mathcal{G}|}(\frac{T_g^M}{T_g^\Omega}) \cdot X_g + \sum_{p=1}^{|\mathcal{A}|}(\frac{T_p^M}{T_p^\Omega}) \cdot X_p]}{[\sum_{g=1}^{|\mathcal{G}|}\frac{X_g}{T_g^\Omega} + \sum_{p=1}^{|\mathcal{A}|}\frac{X_p}{T_p^\Omega}]} \leq (\delta - T_{comm}); \tag{3.39}$$

$$\sum_{g\epsilon\mathcal{G}} X_g + \sum_{p\epsilon\mathcal{A}} X_p \geq 1; \tag{3.40}$$

$$\sum_{g\epsilon\mathcal{G}} X_g + \sum_{p\epsilon\mathcal{A}} X_p \leq |\mathcal{A}| + |\mathcal{G}|. \tag{3.41}$$

Constraint (3.39) is a combination of constraint (3.24) for gliders and an equivalent constraint for PDVs. It assures that time taken by the gliders and PDVs together to complete the mission will be less than the time bound δ. Heterogenous team is the most practical case for time and energy critical missions like rescue of drowning nuclear powered submarine. Gliders have the advantage of being energy efficiency, while PDVs offer the advantage of high speed and maneuverability. Together the two types of AUVs form a potent and flexible combination to accomplish critical missions efficiently in terms of both time and energy. The PDVs act as the primary responders, while the gliders act as sentinels and provide peripheral functionalities. Constraint (3.41) assures that the minimum number of AUVs in the heterogenous team is one. In extreme case, the AUV chosen may be either a glider or a PDV. Constraint (3.40) assures that the maximum number of AUVs chosen is less than or equal to the total available AUVs, i.e., the sum of PDVs and gliders deployed.

3.4 Application: Underwater Acoustic Imaging

One of the applications envisaged in this work is the use of a team of gliders and PDVs that cooperate to complete a specific mission, of *acquiring still images and videos* of an unknown underwater object, within an application-dependent delay bound [32][31]. For this application, gliders are endowed with underwater acoustic imaging systems and use *computer vision techniques and algorithms* to reduce the redundancy of the acquired data.

Underwater imaging technique envisioned in this work is acoustic imaging [15], which produces two dimensional images of underwater objects by transmitting sound waves and detecting reflected waves from the object, as shown in Fig. 3.7. The main advantage of underwater acoustic imaging over optical imaging is the distance of the object from which the images can be obtained. In deep murky sea waters the visibility of optical imaging system decreases drastically. It is in the range of 1 to 3 m, which limits its use. Acoustic energy penetrates the mud and silt that cause optical turbidity in murky waters because the wavelengths of acoustic waves are longer than optical wavelengths [22]. A side scan sonar is a type of acoustic imaging technique that this paper is focusing on [27]. An example of side scan sonar image is illustrated in Fig. 3.7, which indicates the superiority of underwater acoustic imaging over optical imaging.

Figure 3.7: Image of an aeroplane wreck obtained using side scan sonar released by National Oceanic and Atmospheric Administration (NOAA).

Side scan sonar is the technology in which the acoustic wave generating source is placed at one of the side of the glider or the AUV. The side scan sonar is commonly used for imaging objects at the bottom of the sea but it can also be used to image objects that are suspended in the middle of the water body. The acoustic spectrum in which the side scan sonar operates is 0.1 to 1 MHz [22]. The wavelength of the acoustic spectrum is of the order of 0.075 to 1.5 cm. The resolution of an acoustic imaging system is defined as its ability to resolve multiple targets as distinct and separate [23]. It is a function of sonar pulse width, beam spreading, speed of the glider and distance of the glider from the object to be imaged. There are two types of resolution in acoustic imaging systems: 1) *azimuth resolution* (also known as transverse resolution or along track resolution) and 2) *range resolution* (also known as across track resolution).

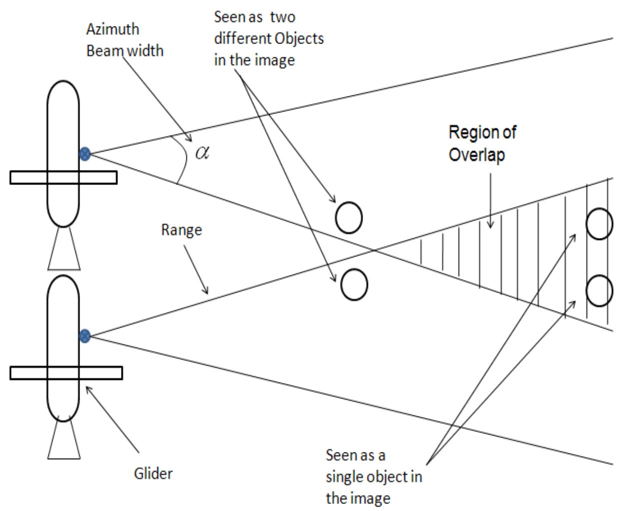

Figure 3.8: Azimuth resolution or transverse resolution is the power to resolve the objects that lie in a line parallel to the path of the glider or the AUV.

1. The *azimuth resolution* is the ability of resolving similar objects that lie in a line parallel to the path of the glider or the AUV. It is the minimum distance between two objects parallel to the line of travel that will be displayed on the sonar as separate objects in the image. This minimum distance is equivalent to the beamwidth (which widens with its distance from the source) at any particular point, as shown in Fig. 3.8. The ability to resolve between objects goes on decreasing as the distance of the glider or AUV from the object goes on increasing [27]. Azimuth resolution ω is given as,

$$\omega = \frac{k \cdot R \cdot \lambda}{L}, \tag{3.42}$$

where k is a constant that depends on shape and size of the receiver, λ [km] is the wavelength of the sonar beam used, L [km] is the length of transmitter/receiver aperture, and R [km] is the radius of the constellation sphere constructed around the target object, as shown in Fig. 3.9. From (3.42), it is observed that the radius R of the *constellation sphere* is limited only by the azimuth resolution required for the mission. The azimuth resolution value, in fact, puts a lower limit R_{min} $[km]$ and upper limit R_{max} $[km]$ on the value R. R_{min} is determined by the near/far (NF) field limit or the NF limit of the underwater acoustic imaging system and all conventional side scan sonar systems operate in the far field. Far field limit is a condition where the acoustic wave front arriving at the aperture can be considered as a plane wave. R_{max} is determined by many factors like the absorbtion of sound in water, salinity, and temperature. The value of R_{max} is provided by the acoustic imaging system manufacturer, and it limits the distance from the target object at which the gliders or AUVs can be positioned for imaging.

2. The *range resolution* is the minimum distance between two objects that lie perpendicular to the line of travel that will be displayed as separate objects. The range resolution is given by the width of the radar pulse width. If the width of the transmitted pulse is τ [s], then the range resolution Δ [m] is given as,

$$\Delta = \frac{c \cdot \tau}{2}, \tag{3.43}$$

where c is the speed of sound in water, which is approximately 1500 m/s [27].

One more assumption is added to the basic model assumptions described in Sect. 3.1, which is specific to the underwater acoustic imaging application. It is given as,

- The area covered S_c at slant range R is determined by the solid angle Υ of the cone that intercepts the half power band width points of the side scan sonar, as shown in Fig. 3.10,

$$S_c = R^2 \cdot \Upsilon, \tag{3.44}$$

with

$$\Upsilon = Q \cdot \alpha \cdot \beta, \tag{3.45}$$

where α and β are the vertical and horizontal beamwidths in radians, respectively,

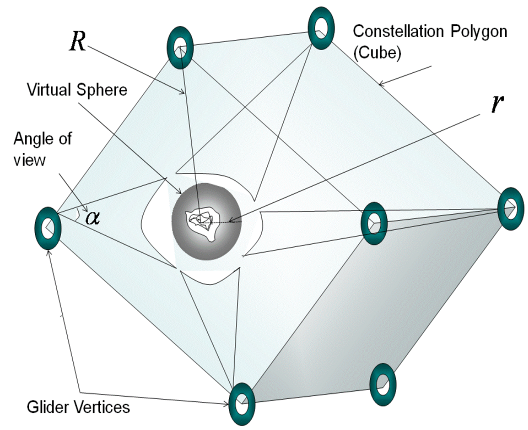

Figure 3.9: Constellation formation to capture object images.

while Q depends on the shape of area covered ($Q = 1$ for rectangular area, $Q = \pi/4$ for circular or elliptical area).

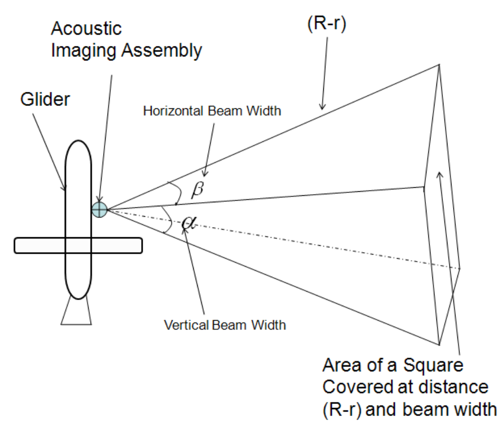

Figure 3.10: Area covered by side scan sonar at a distance (R-r).

Underwater acoustic imaging mission is implemented using the problem formulation and the mathematical model described in Sect. 3.3.

Chapter 4

Performance Evaluation

In this chapter, we evaluate the performance of the task allocation optimization problem formulated for gliders, PDVs and heterogenous team i.e., gliders and PDVs as described in Sect. 3.3, for various scenarios using simulations. In Sect. 4.1, we evaluate the tradeoff between the size of the geocast region and optimality of the solution. In Sect. 4.2, we evaluate the effect of underwater currents on the choice of the geocast region. In Sect. 4.3, we evaluate the localized nature of the problem in absence of underwater currents. In Sect. 4.4, we compare the energy of the team of gliders and PDVs based on the mission length, when the team is deployed for the acoustic imaging mission. In Sect. 4.5, we compare the energy of gliders and PDVs based on the number of vehicles present in the team, when the team is deployed for underwater acoustic imaging mission.

The optimization problem is implemented using $MATLAB^{\circledR}$ and solved using *fmincon* non-linear optimization solver. The AUVs are initially randomly deployed in the 3D underwater region. The parameter values for the glider are set as: the power to operate the buoyancy engine of the glider is 940 W, velocity of the gliders is 6.4 km/hr, C_n has a value of 4, the time for which the buoyancy engine needs to be 'on' to move at a horizontal velocity of 6.4 km/hr is 0.15 hr [41]. The parameter values for the PDVs are set as: the power to operate the propeller engine is 2000 W, velocity varies from 2 to 10 km/hr [14]. The velocity of PDVs is dependent on various non-linear factors like drag force, friction of the motor, etc; hence, the value of non-linear component ζ is set to 0.005. We consider a $10 \times 10 \times 0.2$ km^3 3D underwater region for the deployment of the gliders and AUVs, which is similar to the region off the coast of New Jersey. The object is placed in the center of the region whose coordinates are $(5, 5, 0.1)$ km and diameter of 0.08 km.

The confidence intervals plotted for the simulation results are calculated based on the concept of *Confidence Interval for the Mean* [30]. The selection of a confidence level for an interval determines the probability that the confidence interval produced will contain the true parameter value. Hence, we select a 95% confidence interval so that there is a 95% chance that the simulation results presented in this section will be true. Based on this concept, we calculate 95% confidence intervals for the results. The concept of Confidence Interval for the Mean is explained as follows. An $(1-\epsilon)$ confidence interval for the mean, is an interval (a, b), such that the mean of the population, μ, is inside it (*i.e.*, $a < \mu < b$) with $(1-\epsilon)$ 'confidence'. The end points of the interval, a and b, take values that depend on the random sample selected hence, the confidence interval also depends on the random sample selected. We let $\epsilon = 0.05$ to construct a 95% confidence interval. We use the formula given by,

$$\overline{x} - 1.96 \cdot \frac{\sigma}{\sqrt{n}} < \mu < \overline{x} + 1.96 \cdot \frac{\sigma}{\sqrt{n}}, \tag{4.1}$$

where $\overline{x}$ is the mean, σ is the standard deviation and n is the number of samples.

4.1 Tradeoff Between the Size of Geocast Region and Optimality of the Solution

In this section, we compare the size of the geocast region from which the AUVs are selected with respect to the time required for inter-vehicular communication. The collector needs to collect information from all the AUVs present in the geocast region. The AUVs that are successful in establishing communication with the collector are selected to participate in the optimization problem. Communication involves exchange of information about the position, available energy, their orientation with respect to underwater current, and velocity of underwater current at each AUV. This inter-AUV communication time for exchanging information in turn reduces the total time available to accomplish the mission. The communication is implemented based on the geocasting protocol described in Sect. 3.2. For missions with small time bound this communication overhead can make accomplishing mission impossible.

To observe the actual effect of the size of the geocast region on the optimization problem, underwater currents are not considered in this section. As the size of the geocasting region goes on increasing, more AUVs are available for the mission and this increases the time for collecting the data and solving the optimization problem at the collector. In Fig. 4.1, we observe that the the number of AUVs available to take part in the optimization problem increases with the size of geocasting region. From Fig. 4.2, we observe that the time required for the AUVs to communicate with the collector increases with the size of the geocasting region.

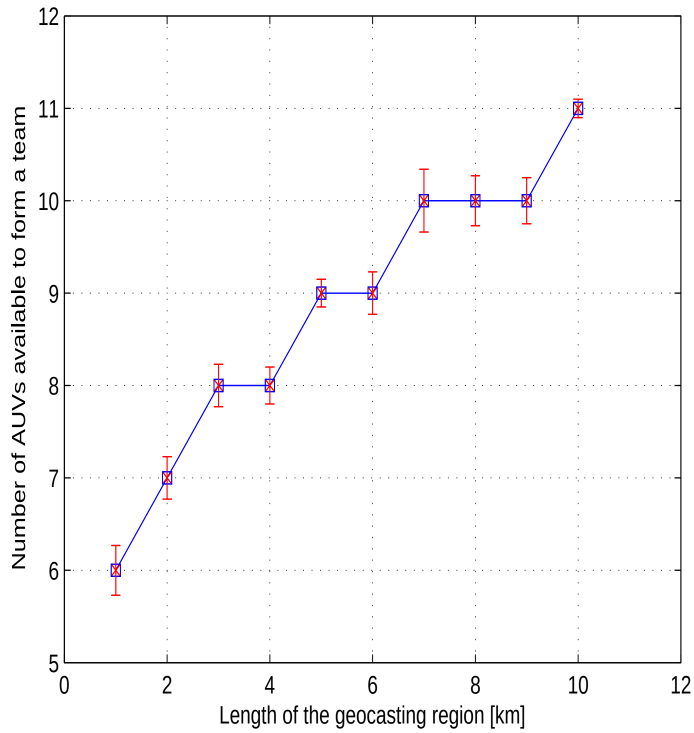

Figure 4.1: Number of vehicles available to take part in optimization problem is shown against length of vector L of the geocast region.

From Fig. 4.3, we observe that the available energy of the team after the mission is the highest when the number of vehicles in the team is five. Now, when the team size is six, suddenly the mission is not feasible. This is due to the fact that time for collecting information from six AUVs causes a communication overhead, which reduces the time available for the mission. It also increases the time required for solving the optimization problem, which in turn reduces the time available for completing the mission and suddenly - even with higher number of vehicles sharing the workload - the mission becomes infeasible.

Hence, choosing a larger region is not always the best solution as it causes a large communication overhead, increases the time to solve the optimization problem, and can make finding the solution to the problem impossible due to insufficient time to complete the mission. Depending on the urgency and time limit for the mission, the algorithm proposed in this work chooses an appropriate number of AUVs in the given geocast region

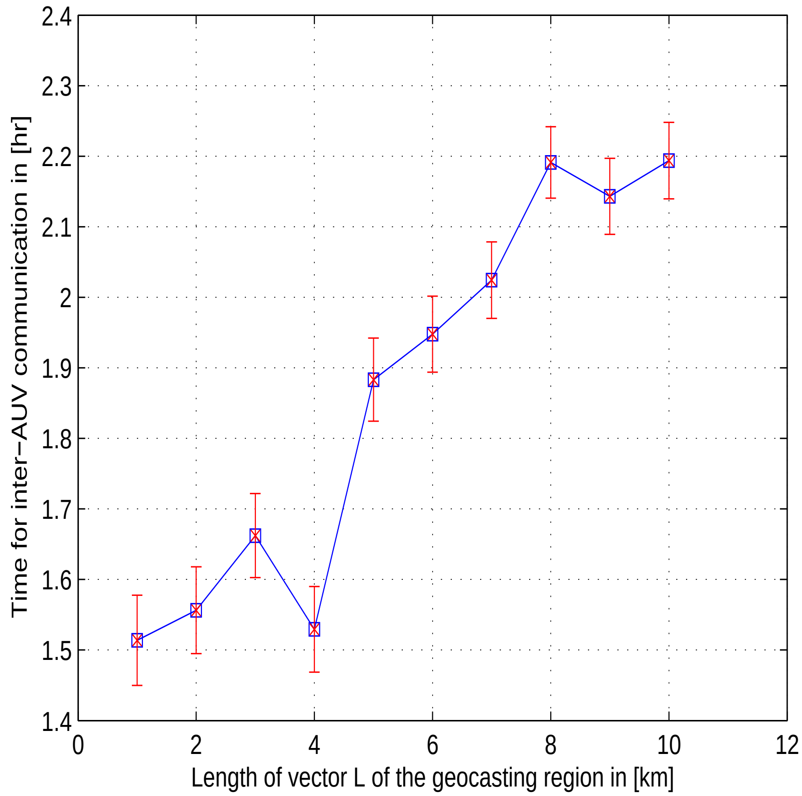

Figure 4.2: Time for communication is shown against length of vector L of geocast region.

to find a feasible and an optimal solution. Other important factor dictating the choice of geocast region is the effect of underwater currents, which is considered in the Sect. 4.2.

4.2 Effect of Underwater Currents on Choice of the Geocast Region

In this section, we analyze how underwater currents affect the choice of the geocast region. As mentioned in Sect. 3.2, the ideal center for choosing the geocast region is the center of target object. The geocast region is chosen symmetrically about the target object in absence of underwater currents; however, when underwater currents are considered, this is not the most efficient choice. In Fig. 4.4, from the Probability Density Function (PDF) we observe that a higher number of AUVs facing the direction of current, i.e., deviating by a small angle α from the direction of underwater currents, are chosen to be a part of the team. Energy is conserved by these AUVs, as they use the force of current to drift along with it, at an increased speed, increasing the energy and time efficiency of the mission. Hence, it is beneficial to chose a geocast region on that side of the target object from where the current is flowing i.e., opposite to the direction of current, rather than choosing it symmetrically

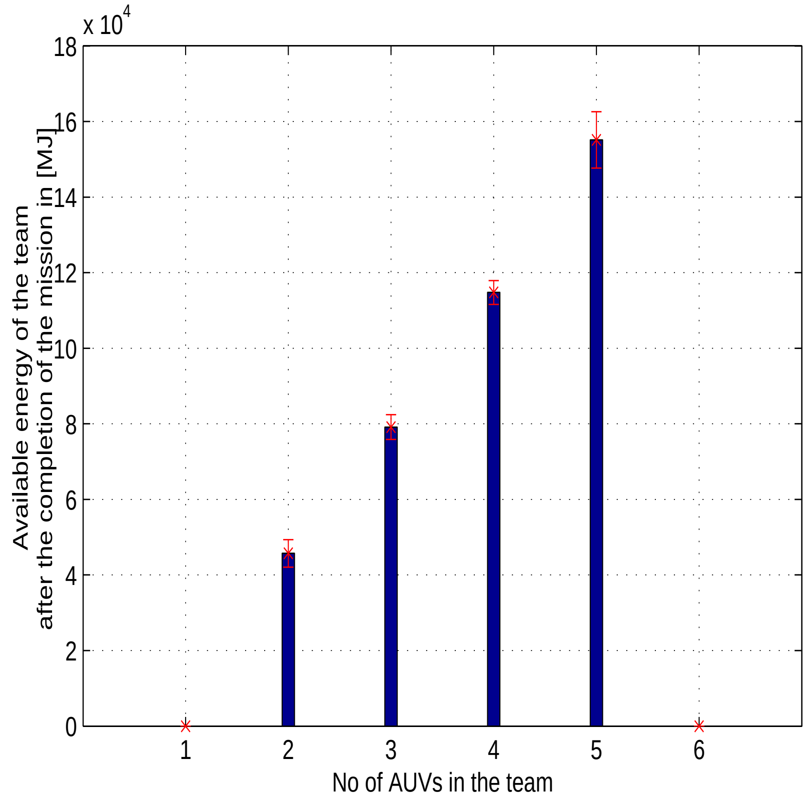

Figure 4.3: Available energy of the team of AUVs after the completion of the mission against the team size.

about it.

4.3 Localized Nature of the Task Allocation Problem

The task allocation problem is localized when underwater currents are not considered. In absence of underwater currents the medium is uniform and all the AUVs have same forces acting on them. Hence, all the AUVs spend same amount of energy to overcome this force. From Fig. 4.5, we observe that the value of the maximum distance from which an AUV is selected to form an optimal team is almost constant as the size of the team goes on increasing.

In contrast, we can observe in Fig. 4.6 that in the presence of underwater currents the distances from which the AUVs are selected are not constant and vary according to the deployment and underwater current patterns. In Fig. 4.4, we see that most of the AUVs selected in the team are the ones that have the lower value for angle α. Thus, it can be inferred from the results that the optimization problem in presence of underwater currents

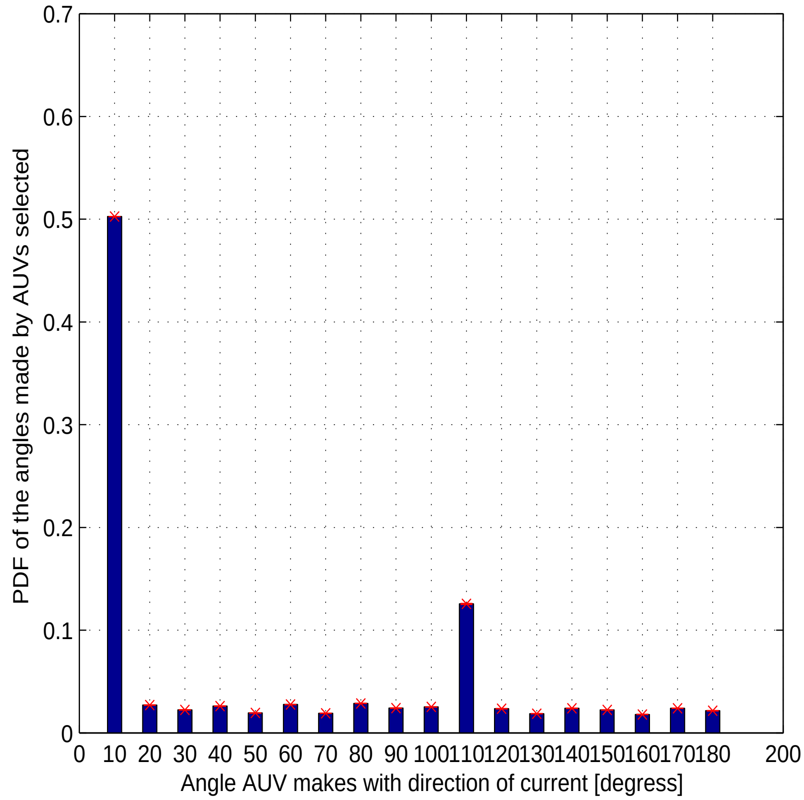

Figure 4.4: Probability Density Function (PDF) of AUVs chosen against the angle α made by them with the direction of the under water current.

is not a localized problem. Hence, the solution of the optimization problem obtained by considering only a subset of AUVs out of all the deployed AUVs is always suboptimal. In Sects. 4.1 and 4.2, we have seen that it is not always possible to consider the entire region of deployment for the optimization problem as it can make the problem infeasible to solve. Hence, the framework proposed in the paper provides a solution that is suboptimal but always feasible.

In Fig. 4.7, we observe that available energy for the team of AUVs does not have linear relationship with the size of the team when underwater currents are considered, as in the case of no underwater currents shown in Fig. 4.3. This can be attributed to the fact that, when moving along with the underwater current, the AUVs tend to use the force of the current to propel themselves at a higher speed but using lower energy. This reduces the energy consumption drastically. Hence, in a real scenario where underwater currents are present, the team with maximum feasible number of AUVs is not always best one.

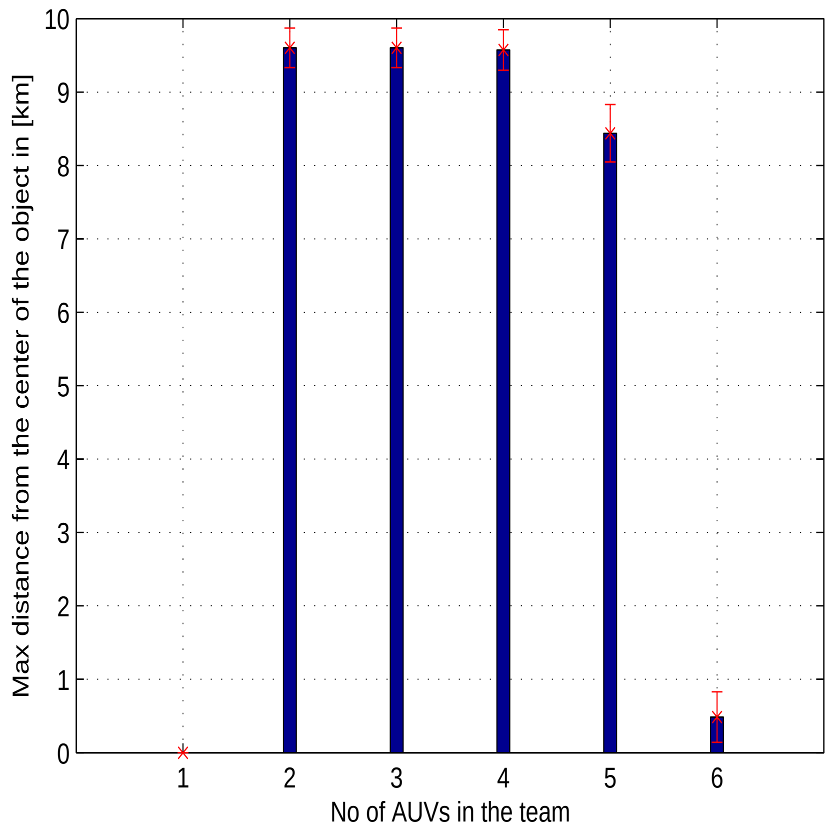

Figure 4.5: Maximum distance from which AUVs are selected in the team is plotted against the size of the team.

4.4 Energy Comparison of Gliders and PDVs Based on Time Bound

In this section, we analyze how the available energy of the team of gliders and PDVs varies with the time bound δ. In Fig. 4.8, we observe that as, the length of the mission goes on increasing (time bound), the energy required by the team of only gliders and only PDVs for the same mission differs. Specifically, the energy of the team of only gliders is comparatively less than that required by the team of only PDVs. PDVs are time efficient as compared to the gliders as we can see from the graph the *infeasible region* for team of PDVs is much smaller than the infeasible region for team of gliders. As the time bound goes on increasing and approaches the feasible region of gliders, the energy difference between the glider team and PDV team is drastic. As seen from the graph, the energy required by the team of 4 PDVs is about 2500 MJ more than that for a team of 4 gliders. Also, a team of 5 PDVs can perform the same work as a team of 6 gliders in less time, but it consumes a greater amount of energy, around 3500 MJ more than the team of 6 gliders. Hence, we can infer

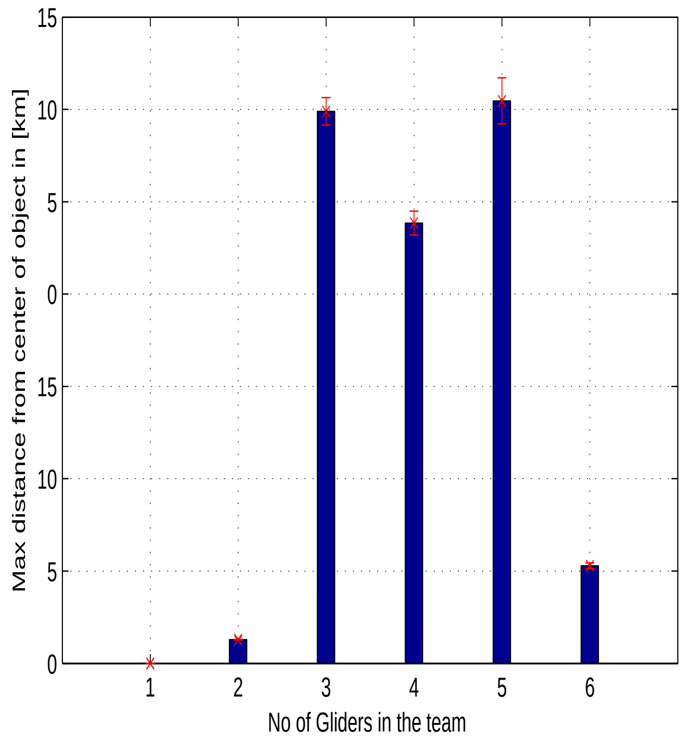

Figure 4.6: Maximum distance from which a AUV is selected against the size of the team in presence of underwater currents.

from the plot that, as a mission length increases, the team of gliders becomes much more energy efficient than the team of PDVs in terms of energy.

From Fig. 4.9, it is observed that, as the mission length goes on increasing, the energy of a team of gliders goes on decreasing. This indicates that, as the mission length goes on increasing, a larger team of gliders has almost the same energy consumption as a smaller team (or even less). From Fig. 4.10, it is observed that, as the mission length increases, the energy for the team of PDVs reaches a constant value. This is the minimum energy required to keep the PDVs afloat and move. Similar to the team of gliders, the energy difference between the larger and the smaller team of PDVs differs by a marginal value. In Fig. 4.8, we observe that the energy of the team of gliders stabilizes at much lower level than that of the team of PDVs. As the energy to scan is much less than that to travel, we conclude that PDVs spend more energy in traveling and keeping themselves afloat at a particular level than gliders. In the case of gliders, the energy to scan is more dominant. This implies that the PDVs as a team consume a very large amount of energy as compared

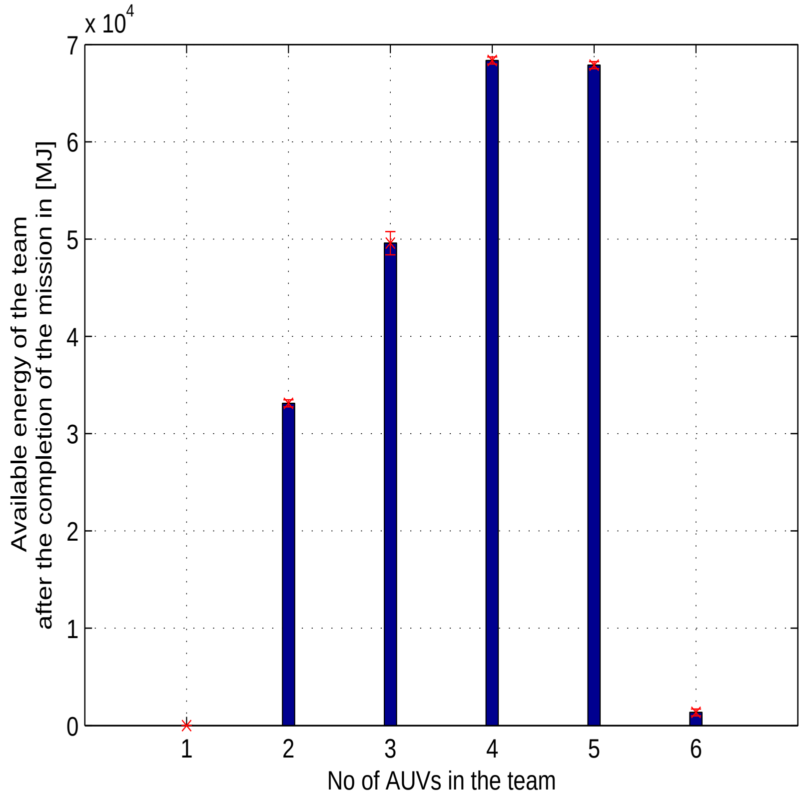

Figure 4.7: Energy of the team of AUVs against the size of the team in presence of underwater current.

to a team of gliders to travel towards the object. This is where the energy efficiency of gliders has its advantage over PDVs in saving energy and cost. From Figs. 4.9 and 4.10, it is observed that as the mission length increases the number of gliders or AUVs selected for the mission decreases. The energy of team of PDVs or gliders also decreases with increase in time bound. Ideally for an infinite time bound, only a single glider would be selected, so that the energy of team would be minimum. The optimization algorithm is run centrally on the computer of one of the glider or a PDV. As the time bound goes on decreasing, the solution of the optimization problem involves more and more vehicles in the proximity of the target object. Hence, an heterogenous team consisting of PDVs and gliders fitted with a variety of sensors would provide a best possible solution in terms of energy and time efficiency. For mission with long distance and mission length, a team with more gliders is preferred, whereas for a mission with long distance and smaller mission length a team with more PDVs is preferred.

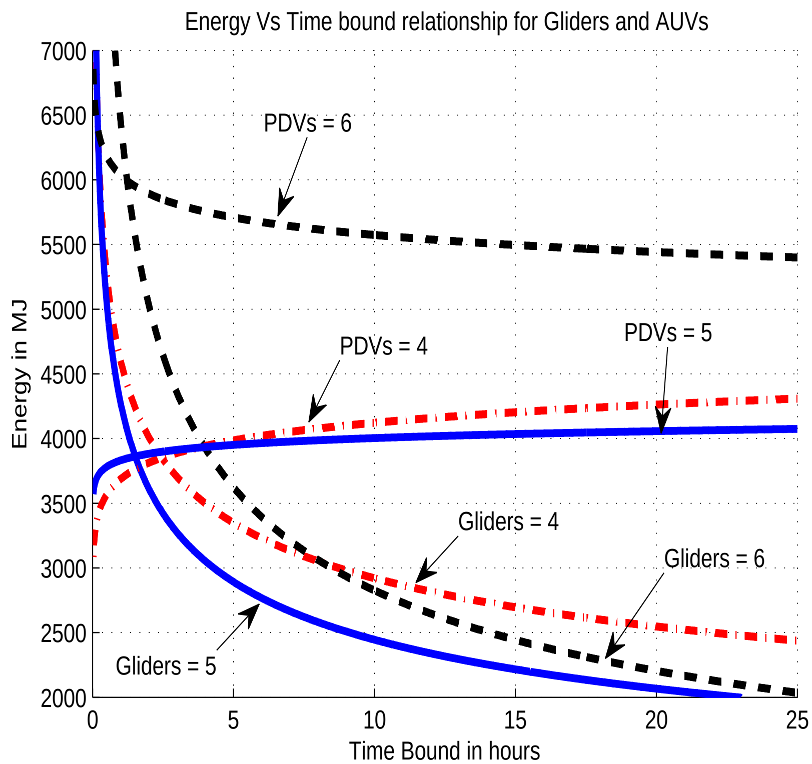

Figure 4.8: Comparison between the energy in MJ of gliders and PDVs vs. the time bound for the mission δ.

4.5 Energy Comparison for Gliders and PDVs Based on the Number of Vehicles Present in the Team

In this section, we show how the total energy of a team of gliders and a team of PDVs varies with the team size. From Figs. 4.11 and 4.12 we observe that as the value of δ goes on decreasing, more and more gliders are required to form the team. From Fig. 4.12 we conclude that, as δ goes below a certain value, the mission becomes impossible to complete using a single glider and at least two gliders are required to complete the mission in the given time bound. A similar scenario for PDVs is indicated in Fig. 4.14. PDVs are fast compared to the gliders, but as the value of δ goes below a certain value it becomes impossible for a single PDV to complete the mission. From Fig. 4.11 and Fig.4.12, we also observe that the total energy of team as the team size varies from 1 to 5 gliders is in the range of 200 to 250 MJ. The energy for same variation in number of PDVs in the team is 1800 to 2000 MJ, as can be seen from Figs. 4.13 and 4.14. We can observe that the energy for same size team of PDVs and gliders differ by around 1600 to 1750 MJ. Also, the energy to travel for PDVs

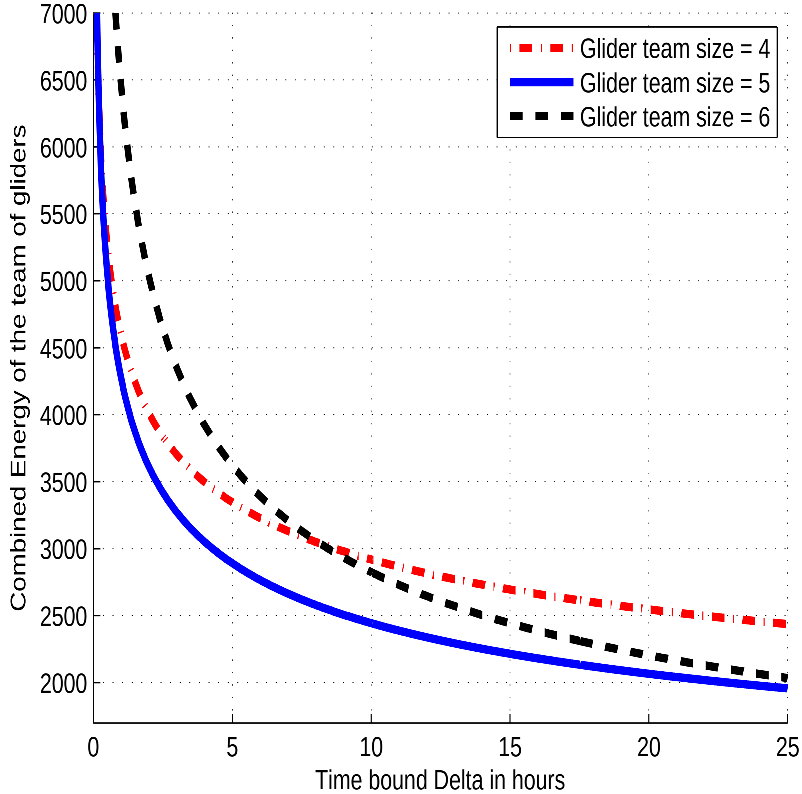

Figure 4.9: Relationship between the energy in MJ of gliders vs. the time bound for the mission δ.

from the initial position to the optimum position, as shown in Figs. 4.13 and 4.14, is more dominant than the energy to scan, which is in contrast to that of team of gliders where energy to scan is very dominant, as can be seen from Figs. 4.11 and 4.12. This implies that the PDVs as a team consume a very large amount of energy as compared to a team of gliders to travel towards the object. This is where the energy efficiency of gliders has its advantage over PDVs in saving energy and cost. For mission with longer distance and longer mission lengths, a team of gliders is preferred over a team of PDVs.

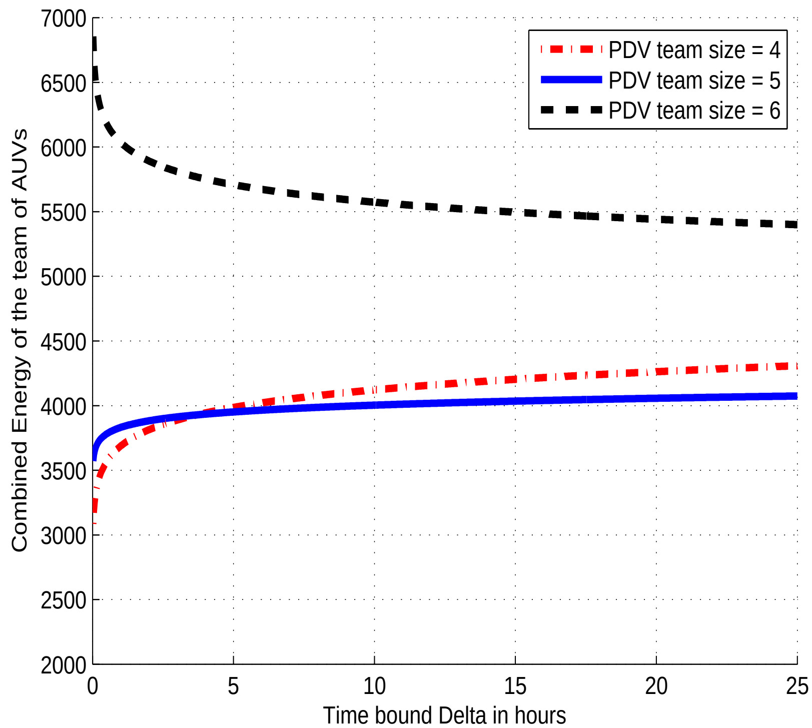

Figure 4.10: Relationship between the energy in MJ of PDVs vs. the time bound for the mission δ.

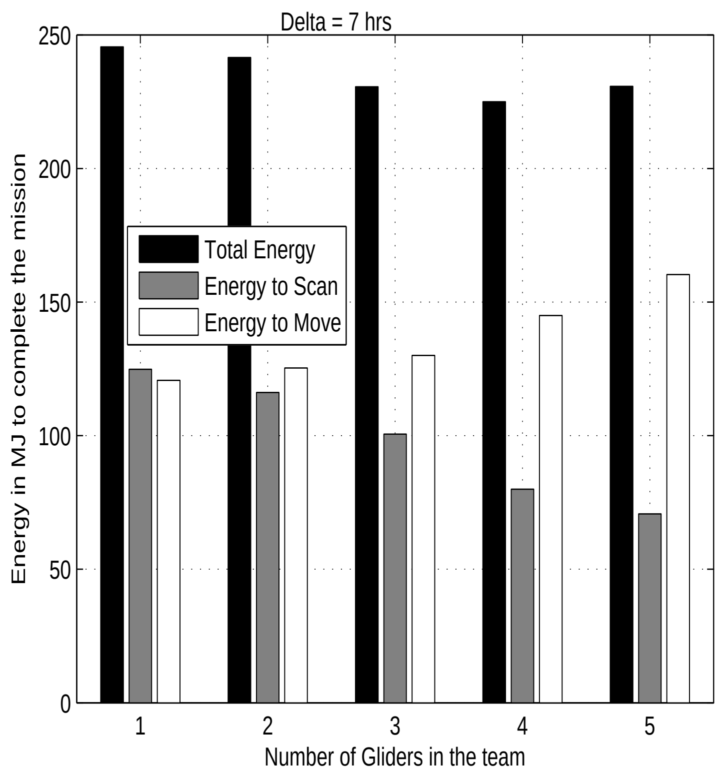

Figure 4.11: Total energy of team of gliders in MJ against the number of gliders in the team when time bound δ is 7 hr.

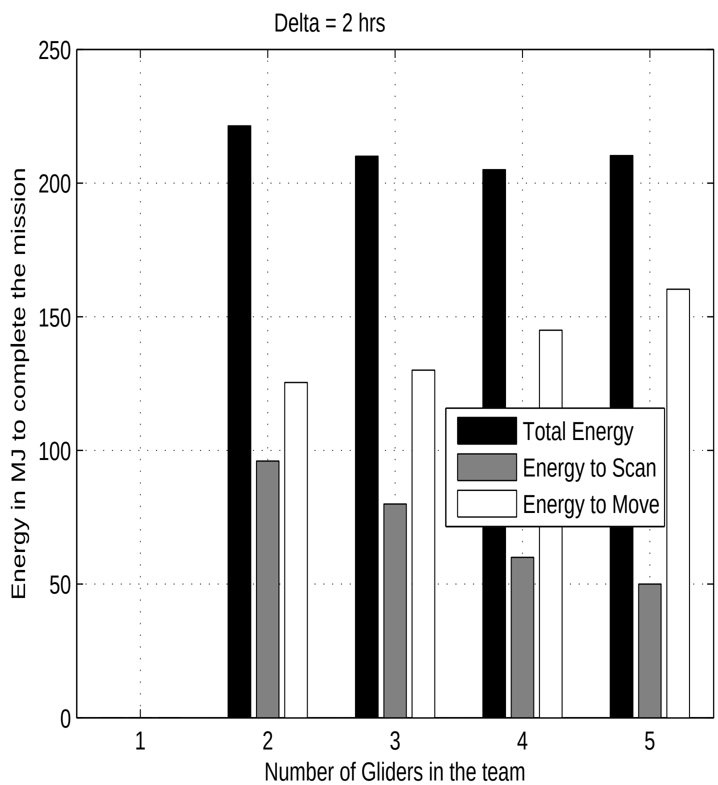

Figure 4.12: Total energy of team of gliders in MJ against the number of gliders in the team when time bound δ is 2 hr.

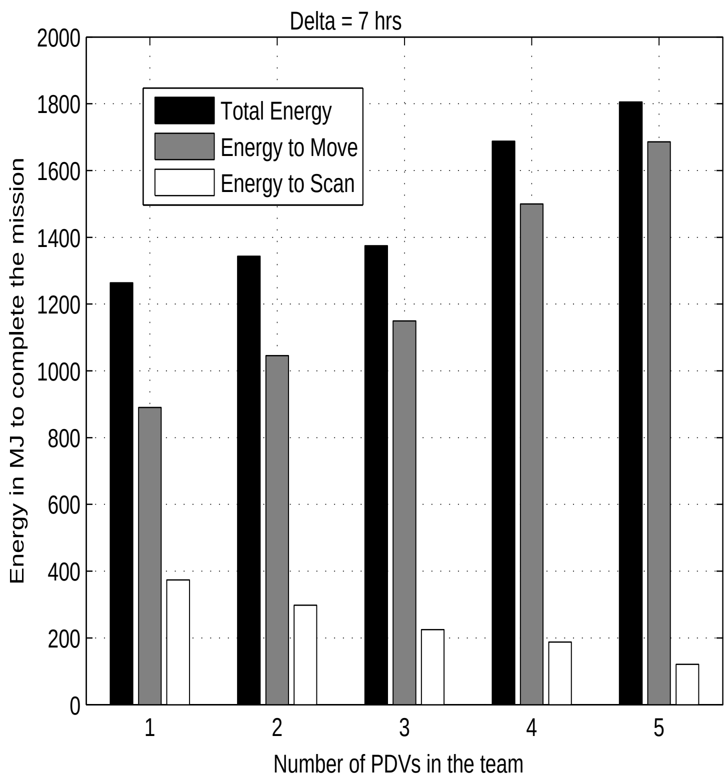

Figure 4.13: Total energy of team of PDVs in MJ against the number of PDVs in the team when time bound δ is 7 hr.

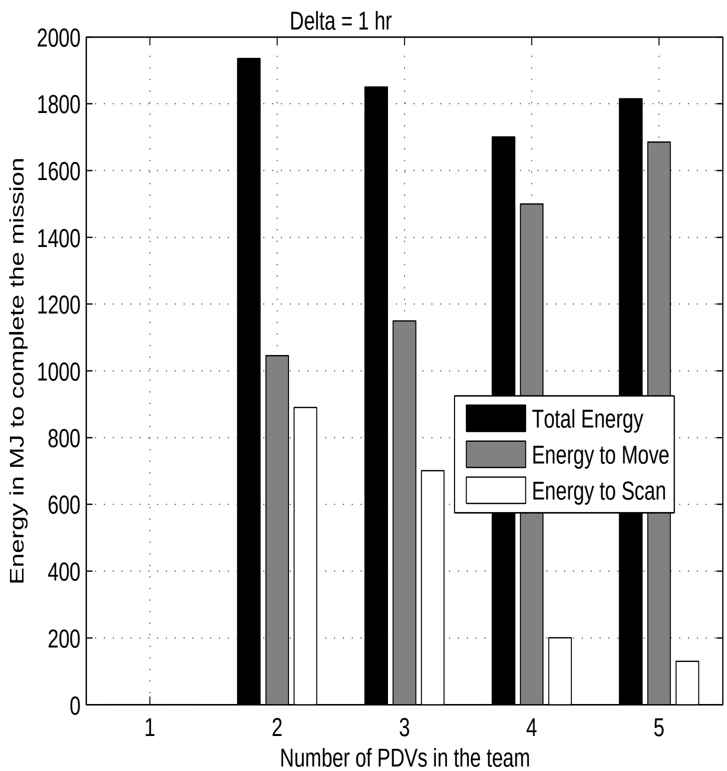

Figure 4.14: Total energy of team of PDVs in MJ against the number of PDVs in the team when time bound δ is 1 hr.

Chapter 5
Conclusion and Future Work

In this chapter, we draw conclusions from the simulation results obtained in Chapter 4 and discuss the scope for future work.

A task allocation framework, to select in a localized manner a best possible team of AUVs to accomplish the mission was developed in this work. The fundamental requirement in any mission is the ability to accomplish the required tasks with reliability and in allotted time. If all the deployed AUVs were selected as a team, the mission may or may not be feasible to accomplish due to the communication overhead and time taken to solve the optimization problem, and even if it were to be accomplished successfully it may be inefficient in terms of resources. Hence, task allocation is required to choose the best possible subset of vehicles in such a way so as to reliably accomplish the mission with high time and energy efficiency. The task allocation is implemented as an optimization problem, which is formulated as *Mixed Integer Non Linear Program (MINLP)*. This optimization problem is solved for various scenarios using $MATLAB^{®}$ and *fmincon* non-linear optimization solver.

From the simulation results we observe that the framework presented allows formation of an optimal team based on task allocation for networked Autonomous Underwater Vehicles (AUVs), capable of accomplishing time critical missions in energy efficient manner. The team formed as a result of this task allocation framework is the subset of all deployed AUVs that is best suited to accomplish the mission while adhering to the mission constraints and time bound. Through simulations, we showed the reliability and the optimality of the results obtained for the proposed framework.

The proposed framework was analyzed using four different criteria, i) the effect of geocast region size on the solution of the optimization problem with special consideration to underwater acoustic communication overhead, ii) the effect of underwater currents on the choice of geocast region, iii) the effect of underwater current on the localized nature of the problem which in turn also affects the choice of geocast region, and iv) the comparison of energy efficiency of team of only gliders with a team of only PDVs with special consideration to team size and mission length.

In Sect. 4.1, we observed the effect of the size of the geocast region from which the AUVs were selected with respect to the time required for inter-vehicular communication. As the size of the geocast region went on increasing, more AUVs were available for the mission and this increased the time for collecting the data and solving the optimization problem at the collector. We also observed that as the team size increased above a certain number the mission suddenly became infeasible. This was due the fact that more AUVs caused a communication over head and increased the time required to solve the optimization problem, which reduced the total time available for the mission.

Hence, we conclude that choosing a larger region is not always the best solution as it causes a large communication overhead, increases the time to solve the optimization problem, and can make finding the solution to the problem impossible due to insufficient time to complete the mission.

In Sect. 4.2, we observed how the underwater currents affected the choice of the geocast region. From the probability density function (PDF), we observed that higher number of AUVs facing the direction of current, i.e., deviating by a small angle α from the direction of underwater currents, were chosen to be a part of the team. Energy was conserved by these AUVs, as they used the force of current to drift along with it, at an increased speed, thus increasing the energy and time efficiency of the mission.

Hence, we conclude that it is beneficial to chose a geocast region on that side of the target object from where the current is flowing rather than choosing it symmetrically about it.

In Sect. 4.3, we observed the the effect of underwater current on the localized nature of the problem which in turn also affected the choice of geocast region. In the presence of underwater currents the distances from which AUVs were selected were not constant and varied according to the deployment and underwater current patterns. Most of the AUVs selected in the team were the ones that had the lower value for angle α. Thus, it can be inferred from the results that the optimization problem in presence of underwater currents is not a localized problem.

Hence, we conclude that the solution of the optimization problem obtained by considering only a subset of AUVs out of all the deployed AUVs is always suboptimal. From Sects.

4.1 and 4.2, we have seen that it is not always possible to consider the entire region of deployment for the optimization problem as it can make the problem infeasible to solve. The framework proposed in the paper provides a solution that is suboptimal but always feasible. The important conclusion is that the optimized solution derived is not only giving the best possible solution, but also a feasible solution, which can be obtained through distributed or localized heuristics.

In Sects. 4.4 and 4.5, we compared the energy of the team of only gliders with the team of only PDVs based on the time bound for the mission and the number of vehicles in the team. We observed that the energy required by the team of gliders was more than the energy required by the team of PDVs and the infeasible time bound for PDVs was much less than that for gliders.

Hence, we conclude that for missions with longer mission length team of gliders is more energy efficient than a team of PDVs but for time critical mission a heterogenous team i.e., glider and PDVs is the best choice.

The time for data collection at the collector AUV can be drastically reduced if one or two hop neighbor knowledge is available. It is an interesting topic for future research to find out the optimality of the suggested geocasting protocol assuming one or two hop neighbor knowledge. Trajectory planning and coordination of the team formed by the task allocation algorithm proposed in this paper is the next step in this research. It can be implemented using the communication and networking frame work suggested in this paper. As the underwater acoustic communication protocols mature the scope for developing highly sophisticated task allocation, trajectory planning and coordination algorithms for AUVs widens.

Appendix A

The time constraint (3.24) can be derived as follows.

Let T_1^{Ω} [hr] be the time required by the first glider to perform the total work Λ [MJ] to complete the mission; the glider rate of work is κ_1^{Ω} [MJ/hr]. Similarly, let T_2^{Ω}, T_3^{Ω}, $\cdots$, T_N^{Ω} be the time required by the remaining $N-1$ gliders and let κ_2^{Ω}, κ_3^{Ω}, $\cdots$, κ_N^{Ω} be their respective rate of work. Hence, we have,

$$T_1^{\Omega} \cdot \kappa_1^{\Omega} = \Lambda, \cdots, T_N^{\Omega} \cdot \kappa_N^{\Omega} = \Lambda,$$

$$\Lambda = \Lambda_1 + \Lambda_2 + \cdots + \Lambda_n.$$

Let T^{Total} be the total time required to complete the mission. Hence,

$$\kappa_1^{\Omega} \cdot T^{Total} = \Lambda_1 \cdots \kappa_N^{\Omega} \cdot T^{Total} = \Lambda_N,$$

$$T^{Total} \leq \delta,$$

$$\Lambda = \tfrac{\Lambda}{T_1^{\Omega}} \cdot (T^{Total} - T_1^M) + \cdots + \tfrac{\Lambda}{T_{n-1}^{\Omega}} \cdot (T^{Total} - T_{n-1}^M) + \tfrac{\Lambda}{T_n^{\Omega}} \cdot (T^{Total} - T_n^M),$$

where T_1^M is the time to reach the target object, $T^{Total} - T_1^M$ is the time the first glider will work alone on the mission until the second glider arrives. Rearranging the terms we obtain,

$$\Lambda = \Lambda[(\tfrac{1}{T_1^{\Omega}} \cdot (T^{Total} - T_1^M)) + \cdots + (\tfrac{1}{T_N^{\Omega}} \cdot (T^{Total} - T_n^M)) + \cdots + (\tfrac{1}{T_n^{\Omega}} \cdot (T^{Total} - T_n^M))],$$

$$[1 + \tfrac{T_1^M}{T_1^{\Omega}} + \tfrac{T_2^M}{T_2^{\Omega}} + \cdots + \tfrac{T_n^M}{T_n^{\Omega}}] = \quad T^{Total}[\frac{1}{T_1^{\Omega}} + \frac{1}{T_2^{\Omega}} + \cdots + \frac{1}{T_n^{\Omega}}]$$

$$\frac{1}{T^{Total}}(1 + \sum_{i=1}^{N} \frac{T_i^M}{T_i^{\Omega}}) \quad = \quad \sum_{i=1}^{N} \frac{1}{T_i^{\Omega}},$$

$$T^{Total} = \frac{1 + \sum_{i=1}^{N} \frac{T_i^M}{T_i^\Omega}}{\sum_{i=1}^{N} \frac{1}{T_i^\Omega}} \leq \delta - T_{comm}.$$

References

[1] http://spray.ucsd.edu/pub/rel/info/spray_description.php.

[2] Explorations, The e-magazine of Scripps Institution of Oceanography, UC, San Diego. http://explorations.ucsd.edu/Features/Landslides/popup/popup_2.php.

[3] Ocean Instruments: How they work, How they do, and why they do it. http://www.whoi.edu/instruments/gallery.do?mainid=16990&iid=1498.

[4] VideoRay. http://www.videoray.com/products/8-explorer.

[5] Woods Hole Science Center Ground-Truth systems. http://woodshole.er.usgs.gov/operations/sfmapping/rov.htms.

[6] A. Howard, M. J. Mataric and G. S. Sukhatme. Localization for Mobile Robot Teams Using Maximum Likelihood Estimation. In *Proc. of IEEE/RSJ International Conference on Robotics and Intelligent Systems (IROS)*, pages 439–459, Laussane, Switzerland, Oct 2002.

[7] Ian F. Akyildiz, Dario Pompili, and Tommaso Melodia. Underwater Acoustic Sensor Networks: Research Challenges. *Ad Hoc Networks (Elsevier)*, 3(3):257–279, May 2005.

[8] Amrita A. Nimbalkar and Dario Pompili. Reliability in Underwater Inter-Vehicle Communications. In *Proc. of ACM International Workshop on UnderWater Networks (WUWNet)*, San Francisco, CA, September 2008.

[9] Ralf Bachmayer, Brad de Young, Christopher Williams, Charlie Bishop, Christian Knapp, and Jack Foley. Development and Deployment of Ocean Gliders on the Newfoundland Shelf. In *Proc. of UVS Canada Conference*, Montebello, Qubec, Nov 2006.

[10] Alexander Bahr, John J. Leonard, and Maurice F. Fallon. Cooperative Localization for Autonomous Underwater Vehicles. *International Journal of Robotics Research*, 28(6):714–728, 2009.

[11] Wolfram Burgard, Dieter Fox, Mark Moors, Reid Simmons, and Sebastian Thrun. Collaborative Multi-Robot Exploration. In *Proc. of IEEE International Conference on Robotics and Automation (ICRA)*, volume 1, pages 476–481, Apr 2000.

[12] D. J. Stilwell, B. E. Bishop. Platoons of underwater vehicles. In *Control Systems Magazine, IEEE*, volume 20, pages 45–52, Dec 2000.

[13] D. O. Popa, A. C. Sanderson, R. J. Komerska, S. S. Mupparapu, D. R. Blidberg, S. G. Chappel. Adaptive Sampling Algorithms For Multiple Autonomous Underwater Vehicles. In *Proc. of Autonomous Underwater Vehicles, IEEE/OES*, pages 108–118. Rensselaer Polytech. Inst., Troy, NY, USA, Jun 2004.

[14] Department of Navy Science and Technology. *AUVSI/ONR Engineering Primer Document for the Autonomous Underwater Vehicle (AUV) Team Competition.*

[15] Donna M. Kocak and Frank M. Caimi. The Current Art of Underwater Imaging With a Glimpse of the Past and Vision of the Future. *Marine Technology Society Journal*, 39(3), 2005.

[16] E. Fiorelli, N. E. Leonard, P. Bhatta, D. Paley, R. Bachmayer, and D. M. Fratantoni. Multi-AUV control and adaptive sampling in Monterey Bay. In *Proc. of Autonomous Underwater Vehicles, IEEE/OES*, pages 134–147, 2004.

[17] Charles. C. Eriksen, T. James Osse, Russel. D. Light, Timothy Wen, Thomas. W. Lehman, Peter. L. Sabin, John. W. Ballard, and Andrew. M. Chiodi. Seaglider: A Long-Range Autonomus Underwater Vehicle for Oceanographic Research. *IEEE Journal of Ocean Engineering*, 26(4):424–436, October 2001.

[18] D. W. Gage. Command Control For Many-Robot Systems. In *Proc. of AUVS Technical Symposium*, pages 22–24, Hunstville Alabama, USA, 1992.

[19] Josuha Grady Graver. *Underwater Gliders: Dynamics, Control and Design.* For the degree of doctor of philosophy, Princeton University, May 2005.

[20] Bo He and Nini Yu. Robot-centered Localization and Map Building for Autonomous Underwater Vehicle. *Computational Intelligence and Natural Computing, International Conference on*, 1:417–420, 2009.

[21] J. G. Graver, R. Bachmayer, N. E. Leonard and D. M. Fratantoni. Underwater Glider Model Parameter Identification. In *Proc. of Unmanned Untethered Submersible Technology (UUST)*, 2003.

[22] Jerry L. Sutton. Underwater Acoustic Imaging. In *Proc. of IEEE*, volume 67, 1979.

[23] John P. Fish. *SOUND UNDERWATER IMAGES A Guide to The Generation and Interpretation of Side Scan Sonar Data.* Lower Cape Publishing, 1990.

[24] Clayton Jones, Elizabeth Creed, Scott Glenn, John Kerfoot, Josh Kohut, Chhaya Mudgal, and Oscar Schofield. Slocum Gliders-A Component of Operational Oceanography. In *Proc. of UUST*. Autonomous Undersea Systems Institute, 2005.

[25] K. Seada, A. Helmy. Efficient and robust geocasting protocols for sensor networks. *Elseiver Computer Communications Journal Special Issue on Dependable Wireless Sensor Networks*, 29(2), Jan 2006.

[26] Dimitrios Katsaros and Yannis Manolopoulos. The Geodesic Broadcast Scheme for Wireless Ad Hoc Networks. In *Proc. of IEEE International Symposium on a World of Wireless, Mobile and Multimedia Networks (WoWMoM)*, Buffalo, NY, August 2006.

[27] William H. Key. Side Scan Sonar Technology. *OCEANS 2000 MTS/IEEE Conference and Exhibition*, 2:1029–1033, 2000.

[28] Indraneel S. Kulkarni and Dario Pompili. Coordination of Autonomous Underwater Vehicles for Acoustic Image Acquisition. In *Proc. of ACM International Workshop on UnderWater Networks (WUWNet)*, San Francisco, CA, Sept 2008.

[29] Indraneel S. Kulkarni and Dario Pompili. Task Allocation for Networked Underwater Vehicles in Critical Missions. *To appear in IEEE Journal of Selected Areas in Communications-Special Issue on Mission Critical Networking (JSAC-MCN)*, 2010.

[30] Ramn V. Len. The Concept of Confidence Interval for the Mean. `http://web.utk.edu/~leon/stat201/Confidence%20Interval%20Concept.html`.

[31] T. Melodia, D. Pompili, V. C. Gungor, and I. F. Akyildiz. Communication and Coordination in Wireless Sensor and Actor Networks. *IEEE Transactions on Mobile Computing*, 6(10):1116–1129, October 2007.

[32] Tommaso Melodia, Dario Pompili, and Ian F. Akyildiz. A Communication Architecture for Mobile Wireless Sensor and Actor Networks. In *Proc. of IEEE Conference on Sensor and Ad Hoc Communications and Networks (SECON)*, volume 1, pages 109–118, Reston, VA, September 2006.

[33] Tommaso Melodia, Dario Pompili, Vehbi C. Gungor, and Ian F. Akyildiz. A Distributed Coordination Framework for Wireless Sensor and Actor Networks. In *Proc. of ACM (Mobihoc)*, Urbana-Champaign, IL, May 2005.

[34] Petter Ogren, Edward Fiorelli, and Naomi Ehrich Leonard. Cooperative Control of Mobile Networks: Adaptive Gradient Climbing in a Distributed Environment. *IEEE Transactions on Automatic Control*, 49(8):1292–1302, August 2004.

[35] Paolo Casari and Albert F. Harris. Energy-Efficient Reliable Broadcast in Underwater Acoustic Network. In *Proc. of ACM International Workshop on Underwater Networks (WUWNet)*, Montreal, Canada, Sept 2007.

[36] Dario. Pompili and Ian. F. Akyildiz. Overview of Networking Protocols for Underwater Wireless Communications. *IEEE Communications Magazine*, 47(1), Jan 2009.

[37] Dario Pompili, Tommaso Melodia, and Ian F. Akyildiz. Routing Algorithms for Delay-insensitive and Delay-sensitive Applications in Underwater Sensor Networks. In *Proc. of ACM Conference on Mobile Computing and Networking (MobiCom)*, Los Angeles, CA, USA, 2006.

[38] Dario Pompili, Tommaso Melodia, and Ian F. Akyildiz. Three-dimensional and Two-dimensional Deployment Analysis for Underwater Acoustic Sensor Networks. *Ad Hoc Networks (Elsevier)*, 7(4):778–790, June 2009.

[39] R. Bachmayer and N. E. Leonard, J. Graver, E. Fiorelli and P. Bhatta and D. Paley. Underwater Gliders: Recent Development and Future Applications. In *Proc. of IEEE International Symposium on Underwater Technology (UT)*, pages 195– 200, Taipei, Taiwan, April 2004.

[40] R. Bachmayer, J. A. Rice, R. Crebert, C. Fletchert. Navigation and Control of Multiple Gliders in an Underwater Acoustic Network. In *Proc. of Autonomous Underwater Vehicles, IEEE/OES*, pages 54–58, Jun 2004.

[41] S. A. Jenkins, D. E. Humphreys, J. Sherman, J. Osse, C. Jones, N. Leonard, J. Graver, R. Bachmayer, T. Clem, P. Carroll, P. Davis, J. Berry, P. Worley, J. Wasyl. Underwater Glider System Study. Technical Report 53, Scripps Institution of Oceanography, May 2003.

[42] Reid G. Simmons, David Apfelbaum, Wolfram Burgard, Dieter Fox, Mark Moors, Sebastian Thrun, and Hakan Younes. Coordination for multi-robot exploration and mapping. In *Proc. of AAAI/IAAI*, pages 852–858, 2000.

[43] R. J. Urick. *Principles of Underwater Sound*. McGraw-Hill, 1983.

[44] Regis Vincent, Dieter Fox, Jonathan Ko, Kurt Konolige, Benson Limketkai, Benoit Morisset, Charles Ortiz, Dirk Schulz, and Benjamin Stewart. Distributed multirobot exploration, mapping, and task allocation. *Annals of Mathematics and Artificial Intelligence*, 52(2-4):229–255, 2008.

[45] Wentao Zhang, Xiaohua Jia and Chuanhe Huang. Energy-Aware Location-Aided Multicast Routing in Sensor Networks. In *Proc. of IEEE International Conference on Wireless Communications, Networking and Mobile Computing (WCNM)*, Wuhan, China, September 2005.

[46] Maren Bennewitz Wolfram, Wolfram Burgard, and Sebastian Thrun. Exploiting Constraints During Prioritized Path Planning for Teams of Mobile Robots. In *Proc. of International Conference on Intelligent Robots and Systems (IROS)*, pages 393–398, 2001.